

**Revisiting the Impact of Targeted vs.  
Blanket Non-Pharmaceutical Intervention Strategies  
in the Early Stages of Epidemic Outbreaks**



Candidate no. 1084701

Submitted in partial completion of the

*Master of Science in Modelling for Global Health*

August 2024

# Abstract

**Background** The COVID-19 pandemic prompted the implementation of drastic non-pharmaceutical interventions worldwide. Population-wide, long-term lockdown had not been considered an appropriate option in the past, even though other diseases like Influenza or SARS-CoV-1 caused substantial death rates among various populations or still do. This raises questions regarding the broader applicability of lockdowns for managing emerging infectious diseases and highlights the importance of exploring alternative strategies that do not rely on widespread restrictions.

**Research Aim** This study aims to identify the drivers of the relative impact of classical targeted interventions compared to blanket strategies.

**Methods** Using an age-structured compartmental model, we simulate different outbreak scenarios in three representative countries and assess the relative impact of the strategies under virological and demographic influences.

**Results** Shielding interventions are more effective if the age-severity curves align with the population structure, making them the preferred strategy for pathogens affecting young and old populations. Asymptomatic transmission seems to be a key determinant of the appropriateness of lockdown strategies. However, the chosen outcome metric strongly influences the preferred intervention strategy. Particularly, we uncover how it is impossible for a strategy to simultaneously be optimal across 3 key indicators: Years of Life Lost (YLL) per death, infection-fatality-ratio and final epidemic size.

**Conclusion** The study suggests blanket strategies are optimal for pathogens with high asymptomatic infectivity. However, targeted strategies can be preferred when a large proportion of the population is high-risk, particularly with low intergenerational mixing

and when intervention timing is critical.

# Contents

<b>List of Figures</b>	<b>vi</b>
<b>List of Tables</b>	<b>viii</b>
<b>1 Introduction</b>	<b>1</b>
<b>2 Materials and Methods</b>	<b>4</b>
2.1 General Model Structure . . . . .	4
2.2 Case Study: Comparison of Shielding and Lockdown Strategies . . . . .	7
2.2.1 Interplay between Demographic and Immunogenic Traits . . . . .	7
2.2.2 Influence of Outcome Metrics Used . . . . .	9
2.3 Multivariate Sensitivity Analysis: Impact of Virological Parameters .	13
<b>3 Results</b>	<b>17</b>
3.1 Comparison of Shielding and Lockdown Strategies . . . . .	17
3.1.1 Interplay between Demographic and Immunogenic Traits . . . . .	19
3.1.2 Influence of Outcome Metrics Used . . . . .	23
3.2 Impact of Virological Parameters . . . . .	26
<b>4 Discussion</b>	<b>30</b>
<b>References</b>	<b>51</b>

## List of Figures

1	<b>Diagram of the Proposed SEIR Model</b> The flow of individuals between model compartments is illustrated here for a generic age group (subscript a). The parameters are described in Table 1, and model equations are given by the set of differential equations above (equations 2 to 8). . . . .	6
2	<b>Population Age Distribution and Contact Matrices Across Three Countries (United Kingdom, Bolivia, South Africa)</b> The upper panels display the population's age structure for each country, with age groups shown on the y-axis and the proportion of the population (%) on the x-axis. The lower panels show age-stratified contact matrices, where the x-axis represents the individual's age and the y-axis represents the age of the contact. The colour gradient indicates the average number of potentially infectious contacts daily contacts, with darker shades representing higher contact frequencies. . . . .	8
3	<b>Age-Severity Curves for the Modelled Pathogen Types</b> The values for IHR (Influenza-like: Table 4 in [1], SARS-CoV-2-like: [2]), HFR (Influenza-like: Table 3 in [1], SARS-CoV-2-like: Table 2 in [3] and CFR (both: [4]) have been obtained from data to account for the typical curve shape of the underlying diseases: Influenza and SARS-CoV-2. . .	15

<b>4</b>	<b>Reduction of Contacts Across Different Countries and Disease Types</b>	
	The line graphs show the effective contact reduction within the total population across three countries and two disease types. Each intervention is evaluated under varying levels of adherence (0.5 to 1.0), with different values for effective intervention coverage (0.7, 0.8, 0.9). . . . .	17
<b>5</b>	<b>Integral of Effective Contact Reduction Across Different Countries and Disease Types</b>	
	The line graphs show the integral of the effective contact reduction according to the scenarios in Figure 4. The integral considers the effective time frame for which the intervention has been active. . . . .	19
<b>6</b>	<b>Average Deaths per 100,000 Population for Influenza and SARS-CoV-2 Across Bolivia, South Africa, and the United Kingdom Under Specific Intervention Scenarios</b>	
	The values are depicted with 95% confidence intervals and are presented on a $\log_{10}$ – scale. . . . .	20
<b>7</b>	<b>Comparison of Impact on Intervention Strategies on YLL per Death and Average Deaths per 100,000 Population Across Different Countries and Diseases</b>	
	This scatter plot illustrates a targeted (red) and broad (blue) intervention strategy on total deaths per 100,000 population ( $\log_{10}$ ) and YLL per death across three countries: Bolivia (circle), South Africa (triangle), and the United Kingdom (square). The disease is represented by lighter symbols (Influenza-like disease) and darker symbols (SARS-CoV-2-like disease) while also showing the effect of varying adherence levels (size of the symbols). . . . .	22

8	<b>Comparison of the Effectiveness of the Intervention Depending on the Outcome Metric Used: Influenza-like Outbreak</b> Each stream displays the outcome for a metric, averaged over the conducted runs, under the interventions (lockdown and shielding) across the three countries (Bolivia, South Africa, and the United Kingdom). . . . .	24
9	<b>Comparison of the Effectiveness of the Intervention Depending on the Outcome Metric Used: SARS-CoV-2-like Outbreak</b> Each stream displays the final outcome for a metric, averaged over the conducted runs, under the interventions (lockdown and shielding) across the three countries (Bolivia, South Africa, and the United Kingdom). . . . .	25
10	<b>Multivariate Sensitivity Analysis of the Predicted Intervention Impact on Total Deaths per 100,000 Population Depending on Disease Type</b> The box plots show the median and interquartile ranges of the reduction in total deaths for all simulated parameter sets. Each parameter set consists of a combination of the values depicted in 4. The simulation exclusively shows the results for the simulation scenario in Bolivia due to its proximity to the intervention's impacts. The intervention configurations have been transferred from the previous analysis setting. . . . .	27
11	<b>Multivariate Sensitivity Analysis of the Predicted Intervention Impact on Total Deaths per 100,000 Population Depending on Disease Type Incorporating Different Relative Infectivities</b> The plot compares the impact of interventions across different levels of asymptomatic (top row) and presymptomatic (bottom row) infectivity for two disease types: Influenza-like (left) and SARS-CoV-2-like (right). . . . .	29

12	<b>Age-Stratified Infection Hospitalisation Ratio (IHR) Scaled to the Total Population for Influenza-like and SARS-CoV-2-like Illnesses Across Bolivia, South Africa, and the United Kingdom</b> The graphs show proportion of the entire population that is expected to be hospitalised due to infection, expressed as a percentage of the total population. The upper panels show the scaled IHR for Influenza-like illness, while the lower panels depict the scaled IHR for SARS-CoV-2-like illness. The y-axis represents the scaled IHR as a percentage of the total population. The annotations in the upper right corner of each panel indicate the population proportion in the identified risk groups (0-10 and 65+ for Influenza-like illness, 65+ for SARS-CoV-2-like illness) for each country. . . . .	31
13	<b>Comparison of Effective Contact Reduction Over Time for Shielding and Lockdown Interventions</b> The plot illustrates both interventions' start and end points, showing the percentage reduction in effective contacts within the total population. The integral as a measure is shown in the hatched areas. As depicted, the calculation accounts for lockdowns that start later than 90 days before the end of the simulation time frame by adjusting the total period. . . . .	64

14	<b>Difference in Deaths per 100,000 Population Between Lockdown and Shielding Interventions Across Bolivia, South Africa</b> The bars represent the average difference in deaths per 100,000 for each country and disease scenario between the interventions. The error bars indicate the standard error of the difference between the two means (Lockdown and Shielding). The values used for the intervention configuration are equal to the ones depicted in Figure 9 and 8. The labels on top of each bar indicate the mean difference deaths per 100,000 population. . . . .	72
----	---	----

## List of Tables

1	<b>SEIR-Model Parameters</b> The relative infectivities of the model are compared to the infectivity of symptomatic, non-severe infections [C - Compartment], which is assumed to be 1. . . . .	7
2	<b>Overview of Contact Patterns and Demographic Structures</b> The table depicts the age distribution and contact patterns in the United Kingdom, Bolivia, and South Africa, determining the choice for the Case Study Scenarios. . . . .	9
3	<b>Summary of Intervention Characteristics Integrated into the SEIR Model</b> The table provides the basic information for implementing the two modelled interventions. . . . .	12

4	<b>Initial Values for the Virological Parameters</b> The calibrated initial values for the model parameters aligned with the published values for the Basic Reproduction Number $R_0$ , Infection-Fatality-Ratio (IFR) and Final Epidemic Size (Z) are displayed. The non-characteristic virological parameters are varied within a range of +- 30%.	13
5	<b>Ranges for the Virological Parameters Used in the SEIR Modelled for Both Disease Types</b>	54
6	<b>Summary of Files for Reproducing the Simulations Conducted Within the Study</b> The table lists all the files needed to execute simulations, with their respective purposes described. All files which have been used to create plots externally from the simulation process (Figure 2, 12, 13, ) can be found in the GitHub in the folder Post_Methodology.	60
7	<b>Summary of External Data Sources for SEIR Model</b> The table lists the external data with their respective source, integrated into the file ModelRuns.xlsx, which provides the base information for the master file.	61
8	<b>Intervention Strategies ranked by Total Deaths per 100,000 Population</b> The result depicts the mean value over the simulation runs conducted with 95% confidence interval (CI) and standard error.	67
9	<b>Intervention Strategies ranked by YLL per Death</b> The result depicts the mean value over the simulation runs conducted with 95% CI and standard error.	68
10	<b>Intervention Strategies ranked by Total Hospitalisations per 100,000 Population</b> The result depicts the mean value over the simulation runs conducted with 95% CI and standard error.	68

11	<b>Intervention Strategies ranked by Final Epidemic Size</b> The result depicts the mean value over the simulation runs conducted with 95% CI and standard error. . . . .	69
12	<b>Intervention Strategies ranked by Infection Fatality Ratio</b> The result depicts the mean value over the simulation runs conducted with 95% CI and standard error. . . . .	69
13	<b>Intervention Strategies ranked by Total Deaths Averted per 100,000 Population</b> The result depicts the mean value over the simulation runs conducted with 95% CI and standard error. . . . .	70

# 1 Introduction

The COVID-19 pandemic prompted the widespread use of extreme non-pharmaceutical interventions (NPIs) to control transmission, particularly in Western countries. Traditionally, epidemiological responses to pandemics focus on contact tracing, isolating the infected, quarantining when necessary, and shielding vulnerable populations. However, the significant proportion of SARS-CoV-2 asymptomatic infections led to the emergency adoption of lockdowns to control transmission and mitigate hospitalisations, marking a substantial divergence from classical public health strategies for respiratory diseases.

Even though diseases like seasonal Influenza cause substantial mortality, particularly among young children [5], they have not prompted similar large-scale lockdowns as seen with SARS-CoV-2. During the 2003 SARS-CoV-1 outbreak, which lacked asymptomatic transmission, lockdowns were not considered necessary, and the pandemic was managed effectively through targeted isolation and quarantining [6, 7]. This raises questions regarding the broader applicability of lockdowns for managing other emerging infectious diseases and highlights the need for evaluating alternative strategies that do not rely on widespread population restrictions.

This study aims to assess the applicability of lockdowns beyond COVID-19 by comparing them with targeted strategies like shielding. A growing body of research shows that changes in social contact patterns can significantly influence the spread of pathogens [8, 9], emphasising the importance of understanding the specific circumstances that require extreme interventions. Age-stratified analyses have become increasingly prominent in assessing the effects of non-pharmaceutical interventions (NPIs) like lockdowns, mask-wearing, social distancing, and quarantining across different age groups [10–13].

These studies suggest that interventions should be tailored according to age-dependent disease severity. To address these findings, this research employs an age-structured computational simulation model to explore the conditions under which a lockdown might be more effective than targeted approaches.

Despite extensive research on NPIs during the COVID-19 pandemic [13–15], a clear gap remains in developing a generalised framework that applies to diverse hypothetical outbreak scenarios. Current analyses often focus on replicating specific pandemic conditions without considering variations in demographic structures, pathogen characteristics, or the interactions between these factors. Additionally, traditional models frequently overlook the population’s age stratification and pathogen age-severity curves, essential for accurately predicting intervention outcomes. For example, Influenza typically follows a U-shaped age-severity curve, putting young children and elderly individuals at high risk [5, 16]. Incorporating these factors into simulation models is essential for accurately estimating the relative impact of different interventions.

Here we use an age-structured SEIR (Susceptible-Exposed-Infected-Recovered) computational model to evaluate the relative effectiveness of targeted versus blanket NPIs during the early stages of an epidemic outbreak. The model aims to develop a generalised framework identifying critical factors guiding intervention strategy selection for a wide range of scenario characteristics. The model simulates various scenarios determined by demographic structure, intervention choice, and pathogen type. By adjusting contact probabilities across different age groups, the study assesses the impact of key variables like population age structure and pathogen-dependent age severity.

Overall, we investigate how demographic and immunogenic factors might influence the preference for specific intervention strategies. It also explores how different met-

rics—such as total deaths and Years of Life Lost (YLL)—affect the optimal choice of interventions for a given setting. Lastly, we conduct a multivariate sensitivity analysis to determine whether these findings are consistent across different diseases, examining whether viral characteristics like asymptomatic transmission mandate one intervention strategy over another.

## 2 Materials and Methods

### 2.1 General Model Structure

Using the programming language R, we implemented a deterministic, age-structured compartmental transmission model, incorporating public health data to analyse the impact of interventions. Within the model, the population is stratified into 5-year age groups from 0 to 100+ years. Individuals transition between the states Susceptible - S, Exposed - E, Infected - I, Recovered - R and Dead - D. The infected compartment I is divided into three different states, where H stands for hospitalised, C for symptomatic, non-severe and A for asymptomatic infections.

The compartments can be summarised as follows:

S: Susceptible individuals

E: Exposed individuals, who are not yet infected

C: Infected, non-severe, symptomatic individuals (Cases)

H: Infected individuals being hospitalised

A: Infected, asymptomatic individuals

R: Recovered individuals

D: Individuals having died because of the disease

The entire population P is susceptible to the disease at the simulation's beginning ( $t=0$ ), except for one exposed index case. The individuals in the population P move between different compartments within the simulation time frame, which is set to 365 days. The total population sum is, therefore, at any time  $t$  of the simulation:

$$P(t) = S(t) + E(t) + C(t) + A(t) + H(t) + R(t) \quad (1)$$

The following ordinary differential equation system summarises the entire transmission dynamics of the extended SEIR model - Figure 1 - with the applied parameters shown in Table 1. The equations below are presented for a generic age group  $a$ , where  $\omega$  describes the ageing factor of people moving from one age group to the contiguous group (when possible).

$$\frac{dS}{dt} = \omega \cdot S - S \cdot \lambda \quad (2)$$

$$\frac{dE}{dt} = \omega \cdot E + S \cdot \lambda - \gamma \cdot E \quad (3)$$

$$\frac{dC}{dt} = \omega \cdot C + \gamma \cdot pc \cdot (1 - IHR) \cdot E - C \cdot v_C \quad (4)$$

$$\frac{dH}{dt} = \omega \cdot H + \gamma \cdot IHR \cdot E - H \cdot v_H \quad (5)$$

$$\frac{dA}{dt} = \omega \cdot A + (1 - pc) \cdot (1 - IHR) \cdot \gamma \cdot E - v_A \cdot A \quad (6)$$

$$\frac{dD}{dt} = \omega \cdot D + v_C \cdot CFR \cdot C + v_H \cdot HFR \cdot H \quad (7)$$

$$\frac{dR}{dt} = \omega \cdot R + v_A \cdot A + (1 - CFR) \cdot v_C \cdot C + v_H \cdot H \cdot (1 - HFR) \quad (8)$$

The equation for the force of infection  $\lambda$  for is given as follows:

$$\lambda = p \cdot \text{Contacts} \cdot \left( \frac{\rho_A \cdot A + \rho \cdot E + C + \rho_H \cdot H}{P} \right) \quad (9)$$

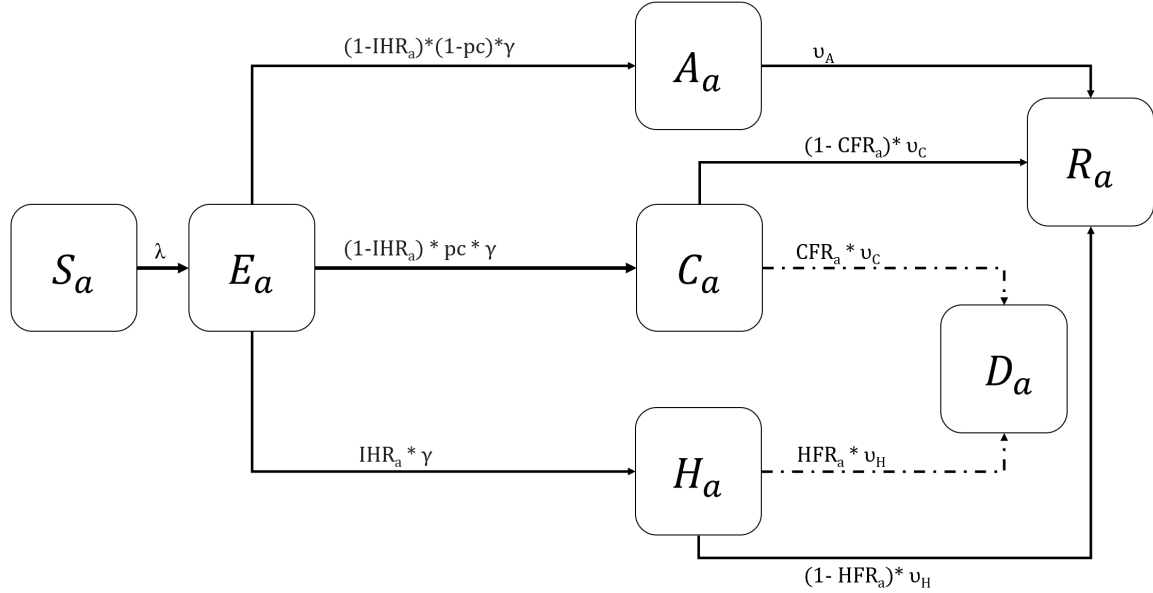


Figure 1: **Diagram of the Proposed SEIR Model** The flow of individuals between model compartments is illustrated here for a generic age group (subscript a). The parameters are described in Table 1, and model equations are given by the set of differential equations above (equations 2 to 8).

**Table 1: SEIR-Model Parameters** The relative infectivities of the model are compared to the infectivity of symptomatic, non-severe infections [C - Compartment], which is assumed to be 1.

Parameter Name	Sign	Unit
Transmission Probability	$p$	/
Probability of Symptomatic Infection	$p_C$	/
Relative Infectivity E	$\rho$	/
Relative Infectivity H	$\rho_H$	/
Relative Infectivity A	$\rho_A$	/
Duration Incubation Period	$\gamma$	$\text{days}^{-1}$
Duration Infectivity C	$v_C$	$\text{days}^{-1}$
Duration Infectivity H	$v_H$	$\text{days}^{-1}$
Duration Infectivity A	$v_A$	$\text{days}^{-1}$
Hospitalization-Fatality-Ratio	HFR	/
Case-Fatality-Ratio	CFR	/
Infection-Hospitalization-Ratio	IHR	/

## 2.2 Case Study: Comparison of Shielding and Lockdown Strategies

### 2.2.1 Interplay between Demographic and Immunogenic Traits

To capture the influence of population age structure, we simulate disease outbreaks in three representative countries: the United Kingdom, Bolivia, and South Africa. These countries were chosen for their distinct demographic profiles and contact patterns, as summarised in Figure 2 and Table 2. Bolivia and South Africa, representing younger populations, are frequently used as examples in the source providing the data for contact matrices [17] due to their distinct contact patterns. The UK is included as a representation of an older population and for its more extensive data availability. This selection allows us to explore the significance of population demographics for varying age severity curves.

The model uses empirical age-dependent contact matrices [17], which inform the num-

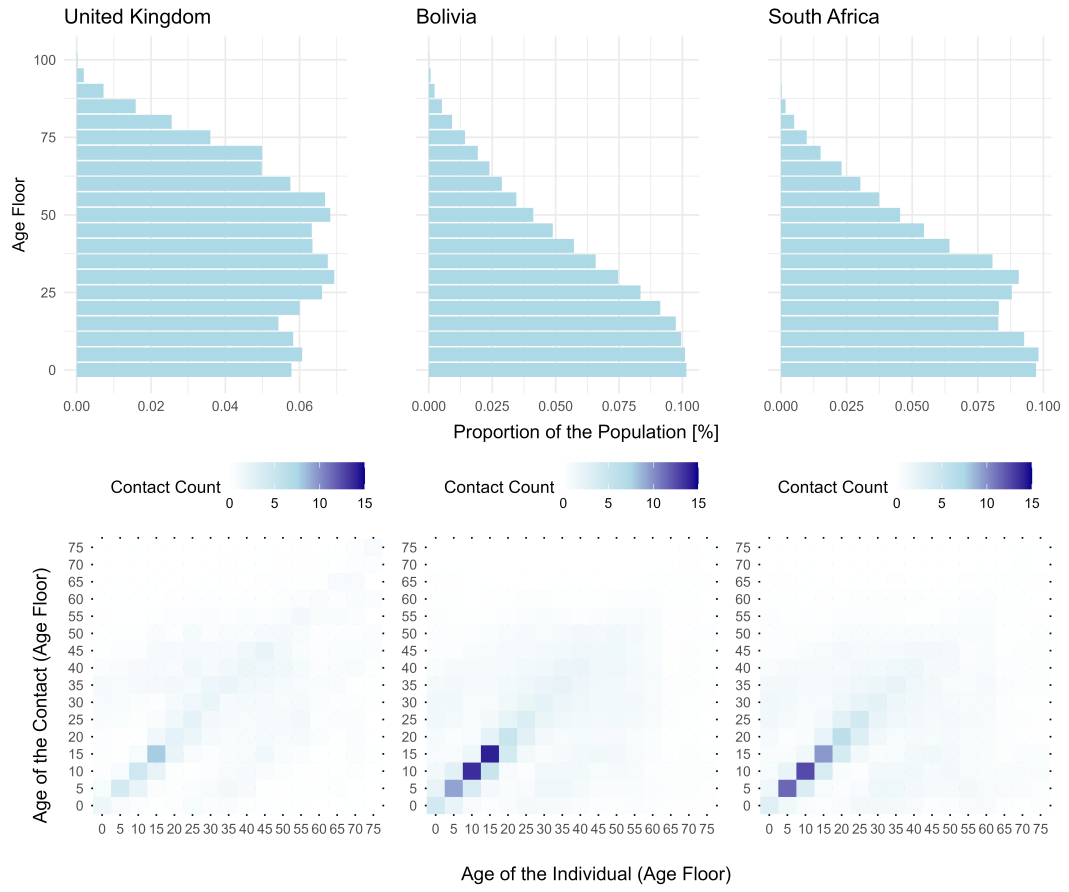


**Figure 2: Population Age Distribution and Contact Matrices Across Three Countries (United Kingdom, Bolivia, South Africa)** The upper panels display the population’s age structure for each country, with age groups shown on the y-axis and the proportion of the population (%) on the x-axis. The lower panels show age-stratified contact matrices, where the x-axis represents the individual’s age and the y-axis represents the age of the contact. The colour gradient indicates the average number of potentially infectious contacts daily contacts, with darker shades representing higher contact frequencies.

ber of potentially infectious contacts across the different age groups for a given population. The data provides contact probabilities for 152 countries, where the population is divided into 16 age groups with a 5-year span (e.g., 0-4 years, 5-9 years, etc.). The model extends the age groups to 21 by copying the contact values from the oldest age group provided by the data. The source offers data for four different environ-

ments—school, work, home, and others — thereby assuming identical contact patterns for everyone over 75. The study design for generating the contact matrices can be found here [17]. The supplementary materials **S2.1** and **S2.2** Data provide further information on the data integration into the SEIR model and the used R-Scripts.

**Table 2: Overview of Contact Patterns and Demographic Structures** The table depicts the age distribution and contact patterns in the United Kingdom, Bolivia, and South Africa, determining the choice for the Case Study Scenarios.

Country	Contact Patterns	Age Demographics
<b>United Kingdom</b>	High contact rates among school-aged children and working adults. The elderly have fewer contacts, mainly within home settings.	High proportion of elderly (18.7% over 65) and moderate proportion of young people (23.1% under 18).
<b>Bolivia</b>	High intergenerational contact, especially within households [17]. Frequent interactions between children, parents, and grandparents.	Relatively young population with many children and young adults (39.9% under 18) and a smaller proportion of elderly (7.5% over 65).
<b>South Africa</b>	Contact patterns vary. High contact among working-age adults in urban areas. In rural areas, there are more interactions within extended families [17].	High proportions of younger and middle-aged individuals (37.1% under 18) and a smaller proportion of elderly (5.5% over 65).

### 2.2.2 Influence of Outcome Metrics Used

The model enables simulating lockdowns as a representative blanket and extreme intervention and shielding as a classical, targeted approach. While the lockdown intervention directly reduces contacts across the entire population, shielding is applied only to the high-risk groups as defined by age-dependent IHR curves. The effective contact reduction (ECR) for the population, caused by intervention x, is given by:

$$\text{ECR}_x = \text{Eff}_x \times \text{Cov}_x \times \text{Adh}_x \quad (10)$$

The efficacy  $\text{Eff}$  is a value between 0 and 1, which indicates how much the contact between the individuals is reduced, given perfect execution, compared to the baseline state given by [17]. The coverage  $\text{Cov}$  indicates what proportion of people follow the intervention  $x$  within the target group. The product of these two values represents the effective coverage, indicating how the intervention would perform in a real-world implementation by reducing infectious contacts at the population level. The adherence factor  $\text{Adh}$  additionally considers how well those following the intervention  $x$  adhere to its protocol. The modified contact matrix, with the adjusted contacts in the population under intervention  $x$ , are given by:

$$\text{Contacts}_x = (1 - \text{ECR}_x) \times \text{Contacts} \quad (11)$$

This is directly applied to the force of infection (Equation (9)). Both interventions have adjustable and fixed parameters that determine their effect on the outcome metrics.

### **Targeted Strategy - Shielding**

Shielding is triggered when a specific percentage of the population is newly infected

daily, which in this model is set at 0.5%, based on the shielding intervention introduced in the UK in January 2021 during the COVID-19 pandemic [18]. After the intervention has started, it remains active until the end of the year. The target group is defined as those at most significant hospitalisation risk. When a sharp rise in the IHR is observed for a particular age group, that group is classified as high-risk and targeted. The IHR is chosen as the most relevant indicator as it reflects the severity of the disease, the associated risk of mortality, and the potential economic burden due to increased use of healthcare capacity. Given the age contact matrices, targeted interventions can have a desirable impact on the transmission dynamics of other age groups that would otherwise have a lot of infectious contact with the target group. For instance, children under five are highly affected by Influenza-like diseases, but because they have frequent contact with 5-10-year-olds, the latter group is also protected.

### **Blanket Strategy - Lockdown**

The lockdown is implemented dynamically, with its start date dependent on the current hospital occupancy due to the respective disease type. The implemented *Hospital Occupancy Threshold* is determined based on the number of available beds per 10,000 individuals in a population, as provided by the UN [19]. If this threshold is reached, the intervention lasts for a defined time frame. An additional delay is incorporated to enhance policy relevance, representing the time from the decision to impose a lockdown to its actual implementation, which is set to one week. Table 3 summarises the key characteristics of the interventions.

**Table 3: Summary of Intervention Characteristics Integrated into the SEIR Model**

The table provides the basic information for implementing the two modelled interventions.

Metric	Shielding	Lockdown
<b>Trigger</b>	Daily Prevalence	Hospital Occupancy
<b>Start Value</b>	0.5% of the Population being infected daily	10% of Hospital Beds being occupied by Disease X
<b>Duration</b>	Until last time step	90 days
<b>Target Groups</b>	Risk Groups <i>Influenza-like Disease: 0-10 and 65+ SARS-CoV-2-like Disease: 60+</i>	Entire Population
<b>Contacts affected</b>	Home, School, Work and Other (according to [17])	School, Work and Other (according to [17])

Throughout this dissertation, we will compare these two described transmission control interventions for two major pathogen types: Influenza-A-like and SARS-CoV-2-like disease. Table 4 summarises the parameter values assumed for each disease type. The disease-identifying parameters are asymptomatic infectivity ( $\rho$ ,  $\rho_A$ ) and the probability of symptomatic infection (pc). These choices and the pathogen calibration process are explained in detail in section 2.3.

**Table 4: Initial Values for the Virological Parameters** The calibrated initial values for the model parameters aligned with the published values for the Basic Reproduction Number  $R_0$ , Infection-Fatality-Ratio (IFR) and Final Epidemic Size ( $Z$ ) are displayed. The non-characteristic virological parameters are varied within a range of  $\pm 30\%$ .

Para-meter	Influenza -like-Disease	Source	SARS-CoV-2 -like-Disease	Source	Variation
$p$	0.03	est. from $R_0$	0.042	est. from $R_0$	/
$p_c$	0.8	[20–23]	0.65	[24–27]	/
$\rho$	0.21	[28–30]	0.5	[31–33]	/
$\rho_A$	0.05	[29, 34]	0.4	[35–37]	/
$\gamma$	1	[38, 39]	1/3	[31–33]	$\pm 30\%$
$\rho_H$	1.1	[40]	0.8	[41]	$\pm 30\%$
$v_H$	1/10	[28]	1/9	[31–33]	$\pm 30\%$
$v_A$	1/4	[42]	1/5	[31–33]	$\pm 30\%$
$v_C$	1/5	[43]	1/6	[44, 45]	$\pm 30\%$
<b>Result Characteristics</b>					
$R_0$	1.48	[46, 47]	2.91	[48–50]	/
IFR	0.12 %	[51]	1.2 %	[52]	/
$Z$	60.50 %	/	89.57 %	/	/

## 2.3 Multivariate Sensitivity Analysis: Impact of Virological Parameters

After estimating the conditions under which classical targeted strategies are preferable to blanket interventions, we assess the robustness of the findings through a sensitivity analysis of the virological parameters. In contrast to the simulation runs for the case study, the multivariate sensitivity analysis varies all virological parameters. This way, the output's sensitivity to each parameter can be estimated. Apart from this, the simulation setup is the same as the case study's.

The pathogens model calibration is orientated on two common diseases: Influenza (the most common seasonal type A [53]) and SARS-CoV-2. The choice of these viruses

is guided by incorporating **different relative infectivities** of the asymptomatic  $\rho_a$  and presymptomatic  $\rho$  infections. Individuals exposed to Influenza-like diseases have minor to no presymptomatic or asymptomatic infections. In the case of the SARS-CoV-2-like disease, individuals can spread the virus in all stages, with significantly higher relative infectivities. The values used for the virological parameters within this study have been aligned with the literature and are depicted in Table 4. The script for the model calibration and the ranges obtained from the literature can be found in **S1.1 Methods**.

The disease types are also characterised by **different age-severity curves**. Influenza-like pathogens typically show a U-shaped curve - Figure 3 - indicating that individuals aged 0-5 and 65+ are at significantly higher risk of severe infection than other age groups. In contrast, SARS-CoV-2-like pathogens show a severity curve that increases constantly with age, with individuals aged 60 and above at the highest risk. The data for the age-fatality curves is based on public health data (see Figure 3).

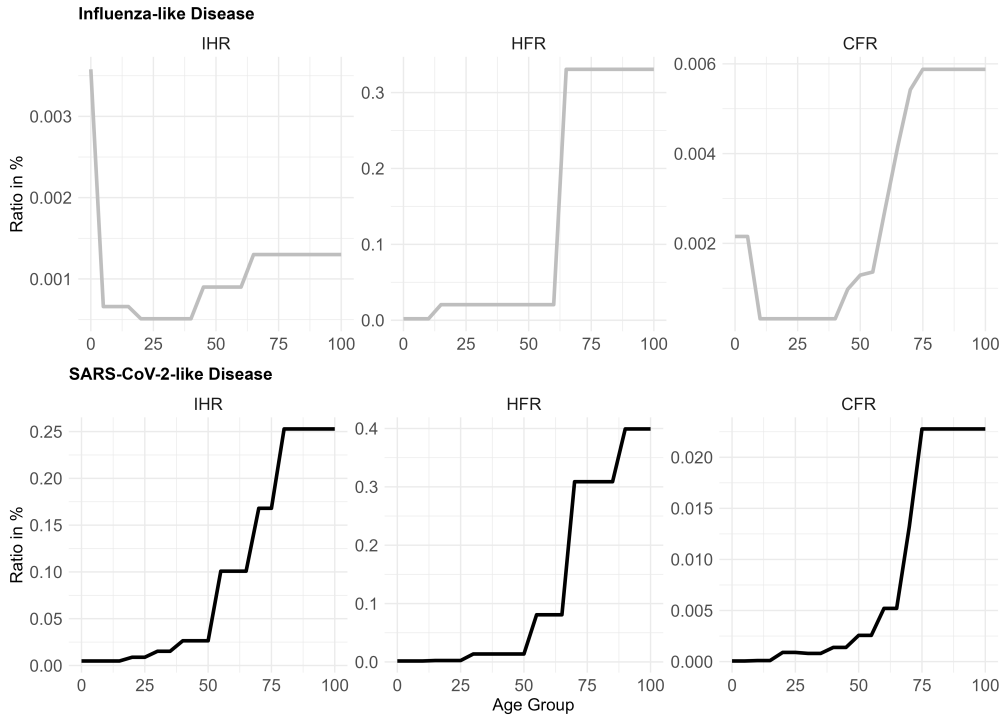


**Figure 3: Age-Severity Curves for the Modelled Pathogen Types** The values for IHR (Influenza-like: Table 4 in [1], SARS-CoV-2-like: [2]), HFR (Influenza-like: Table 3 in [1], SARS-CoV-2-like: Table 2 in [3] and CFR (both: [4]) have been obtained from data to account for the typical curve shape of the underlying diseases: Influenza and SARS-CoV-2.

Overall, as visible in Equations (2) to (8), nine virological parameters and three ratios characterise the disease's spread. Baseline parameters for each pathogen type have been calibrated by matching the simulation outcomes to the pathogen-specific IFR, Basic Reproduction Number ( $R_0$ ) and the Final Epidemic Size  $Z$  (Table 4).  $R_0$  has been estimated according to [54, 55] for an SEIR-model:

$$R_0 = (1 + r \cdot D_I) \cdot (1 + r \cdot D_E) \quad (12)$$

with

$$r = \frac{\log(2)}{T_d}. \quad (13)$$

$T_d$  being the doubling time,  $D_I$  the duration of the weighted average duration of the infectious period and  $D_E$  the duration of the latent period. Further elaboration on the calculation steps can be found in the **S1.2 Methods**.

### 3 Results

#### 3.1 Comparison of Shielding and Lockdown Strategies

##### Comparison of Reduction in Transmission Potential

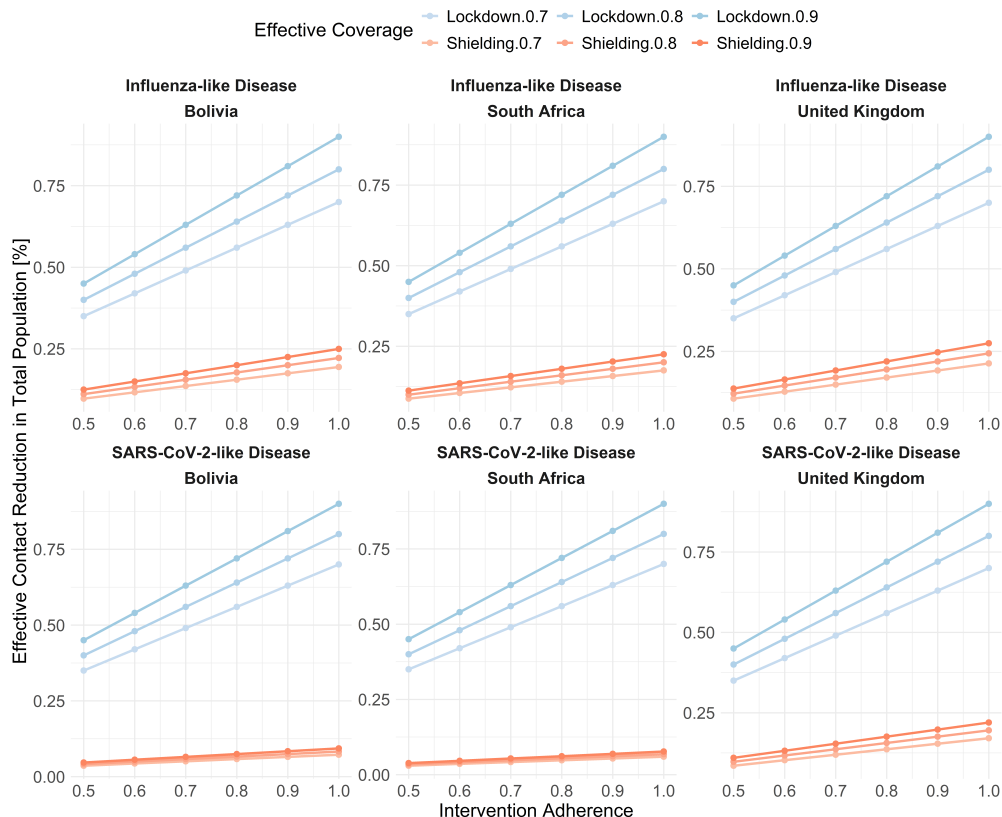


**Figure 4: Reduction of Contacts Across Different Countries and Disease Types** The line graphs show the effective contact reduction within the total population across three countries and two disease types. Each intervention is evaluated under varying levels of adherence (0.5 to 1.0), with different values for effective intervention coverage (0.7, 0.8, 0.9).

Lockdown consistently demonstrates superior results across all scenarios when assessing these strategies' impact on the pathogen's transmission potential across the entire population. Higher adherence to interventions markedly enhances contact reduction,

particularly in the case of lockdowns. Because shielding focuses solely on protecting high-risk groups, it can reduce contacts, depending on the country, by approximately 24-27%. By contrast, lockdown, which does not apply to home contacts, can achieve up to an 86% reduction.

### **Comparison of Reduction in Transmission Potential concerning Time of Intervention Activation**

Analysing the Integral of Effective Contact Reduction, the results reveal scenarios where the impacts of lockdowns and shielding overlap. This result value captures the magnitude and duration of contact reduction the intervention achieves. A more detailed explanation can be found in **S3.1 Results**. Lockdowns reduce contacts more effectively during a SARS-CoV-2-like outbreak; shielding is identified as the preferred strategy during an Influenza-like outbreak. Additionally, the model indicates that a lockdown would not be implemented during an Influenza-like outbreak in South Africa and the United Kingdom as the daily hospitalisation occupancy remains below the critical threshold.

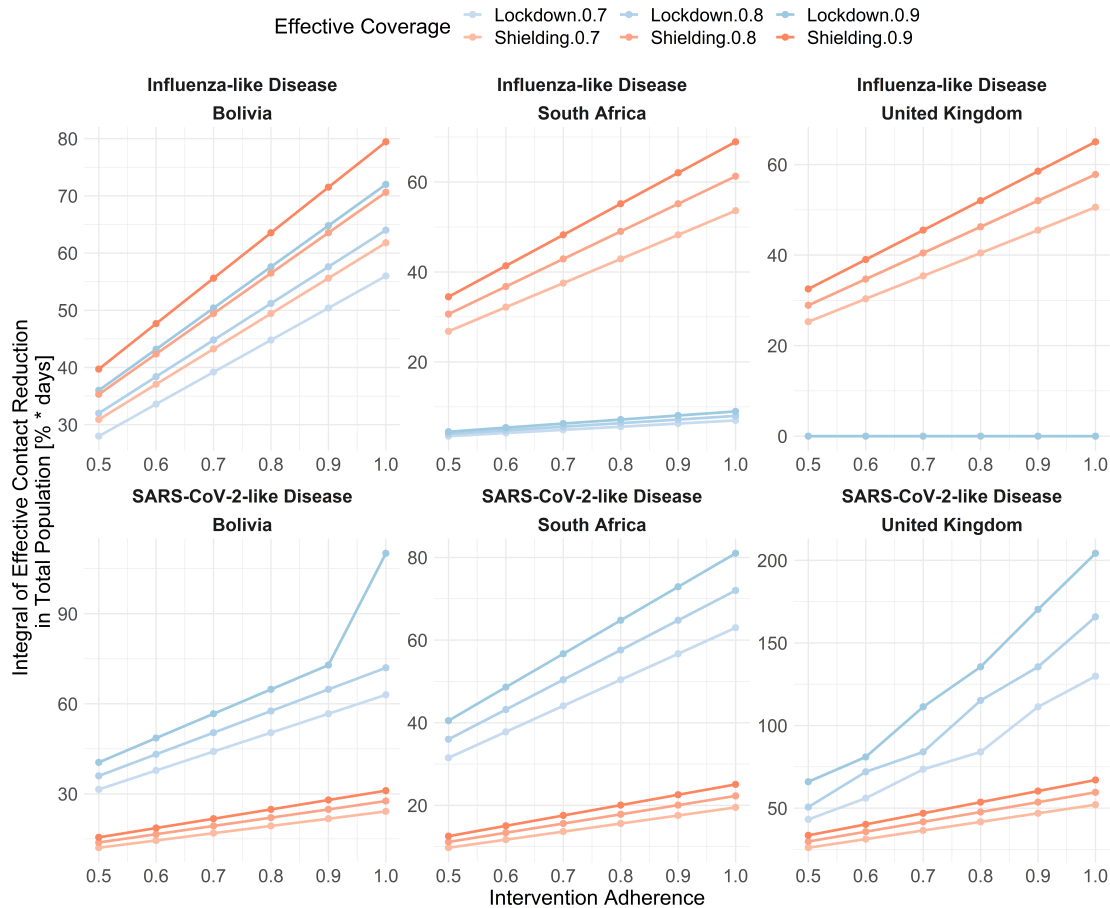


**Figure 5: Integral of Effective Contact Reduction Across Different Countries and Disease Types** The line graphs show the integral of the effective contact reduction according to the scenarios in Figure 4. The integral considers the effective time frame for which the intervention has been active.

### 3.1.1 Interplay between Demographic and Immunogenic Traits

Analysing the metric of total deaths per 100,000 population shows that the strategies' effectiveness becomes more comparable in certain scenarios, depending on their effective coverage and adherence.

For Influenza-like diseases, shielding shows a similar effect across all countries, reduc-

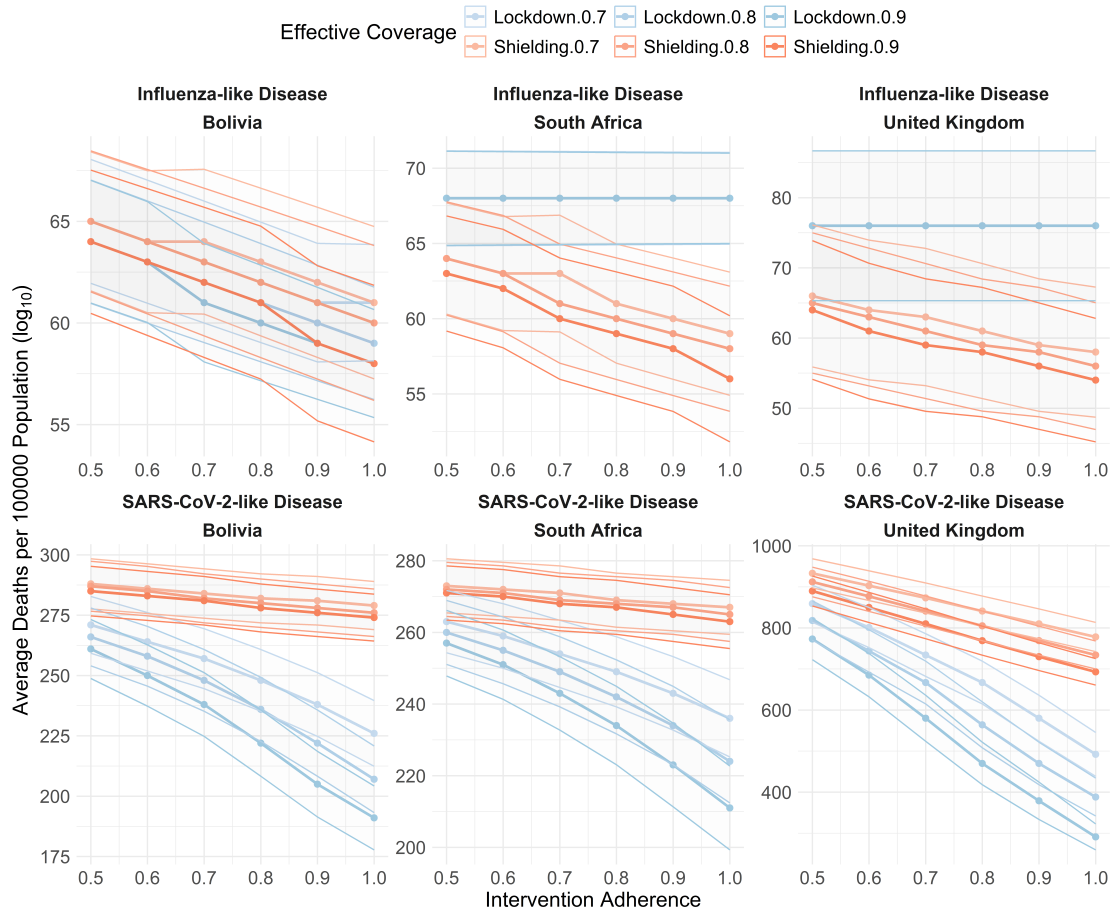


**Figure 6: Average Deaths per 100,000 Population for Influenza and SARS-CoV-2 Across Bolivia, South Africa, and the United Kingdom Under Specific Intervention Scenarios** The values are depicted with 95% confidence intervals and are presented on a  $\log_{10}$  – scale.

ing total deaths per 100,000 by approximately 10, with increasing adherence. Lockdown shows a similar effect in Bolivia and none in the other nations due to the low number of hospitalisations.

For the SARS-CoV-2-like disease, lockdowns death numbers range from 225 to 300 per 100,000 in the population in Bolivia. In South Africa, deaths drop from 240 to 280. In the UK, lockdowns have the most significant impact, decreasing deaths from 700 to 900

per 100,000. Shielding averts about 25 deaths per 100,000 people in Bolivia and South Africa. In the UK, shielding decreases the number in the range from 800 to 900 per 100,000.

Shielding tends to show greater effectiveness in Influenza-like scenarios, while lockdowns are generally more effective in SARS-CoV-2-like scenarios. However, there are notable overlaps between the strategies, particularly in Bolivia during an Influenza-like outbreak and in the United Kingdom during a SARS-CoV-like outbreak. The results show that the impact of shielding and lockdown strategies becomes more comparable in specific scenarios, influenced by effective coverage and adherence levels. Figure 7 compares the relevant intervention configurations over two relevant outcome metrics for each scenario.

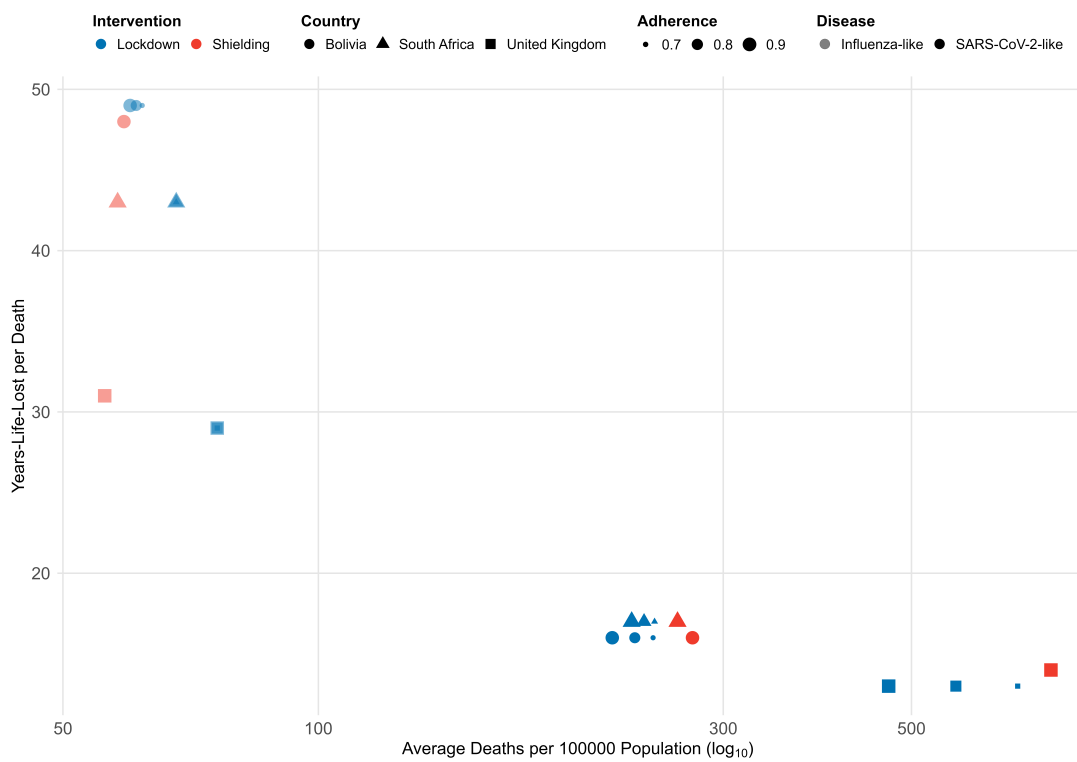


**Figure 7: Comparison of Impact on Intervention Strategies on YLL per Death and Average Deaths per 100,000 Population Across Different Countries and Diseases**

This scatter plot illustrates a targeted (red) and broad (blue) intervention strategy on total deaths per 100,000 population (log<sub>10</sub>) and YLL per death across three countries: Bolivia (circle), South Africa (triangle), and the United Kingdom (square). The disease is represented by lighter symbols (Influenza-like disease) and darker symbols (SARS-CoV-2-like disease) while also showing the effect of varying adherence levels (size of the symbols).

The graph confirms that lockdown strategies are generally more effective in reducing mortality. Both strategies show similar YLL values during SARS-CoV-like outbreaks (ranging from 13 to 17) across all countries.

In Influenza-like outbreaks, shielding consistently reduces mortality more effectively than lockdown across all nations; for YLL, shielding results in higher values in the UK, similar values in South Africa, and lower values in Bolivia.

### **3.1.2 Influence of Outcome Metrics Used**

Derived from Figure 7, the intervention strategies can have a similar impact when lockdown adherence is lowest. The most similar configurations were selected and ranked according to the metrics [Shielding (Eff.Cov.: 90%, Adh.: 90%), Lockdown (Eff.Cov.: 80%, Adh.: 70%)].

The figure shows that shielding in Bolivia, South Africa, and the UK leads to higher total deaths averted (9, 11, and 20 per 100,000, respectively) and fewer deaths per 100,000 (5, 58, 56) compared to lockdowns in an Influenza-like outbreak. The shielding strategy in the UK results in the lowest epidemic size (0.503) and the total deaths per 100,000 (56).

The figures demonstrate that shielding is generally the preferred strategy for Influenza-like diseases. However, there are two exceptions: (1) In the UK, lockdowns can result in lower YLL per death compared to shielding, and (2) in Bolivia, lockdowns lead to a smaller final epidemic size. Despite these exceptions, shielding tends to be more effective in reducing the infection-fatality ratio, particularly in South Africa and the United Kingdom.

In contrast, during the SARS-CoV-2 outbreak, there is a clear trend favouring lockdowns as the preferred intervention. Notably, there are two metrics where both interventions show similar effects: (1) YLL per death differs by only one in South Africa and Bolivia. (2) The IFR can be reduced more by shielding in the UK (0.867 % vs 1.018 %) and is similar in South Africa (0.277% vs 0.288 %). In South Africa, both interventions show similar effects in reducing total deaths (shielding: 248 vs lockdown 276 per 100,000), but lockdowns remain more effective. Detailed rankings for all outcome metrics, with

### Influenza-like Outbreak

(Lockdown Adherence: 0.7, Shielding Adherence: 0.9, Lockdown Effective Coverage: 0.8, Shielding Effective Coverage: 0.9)

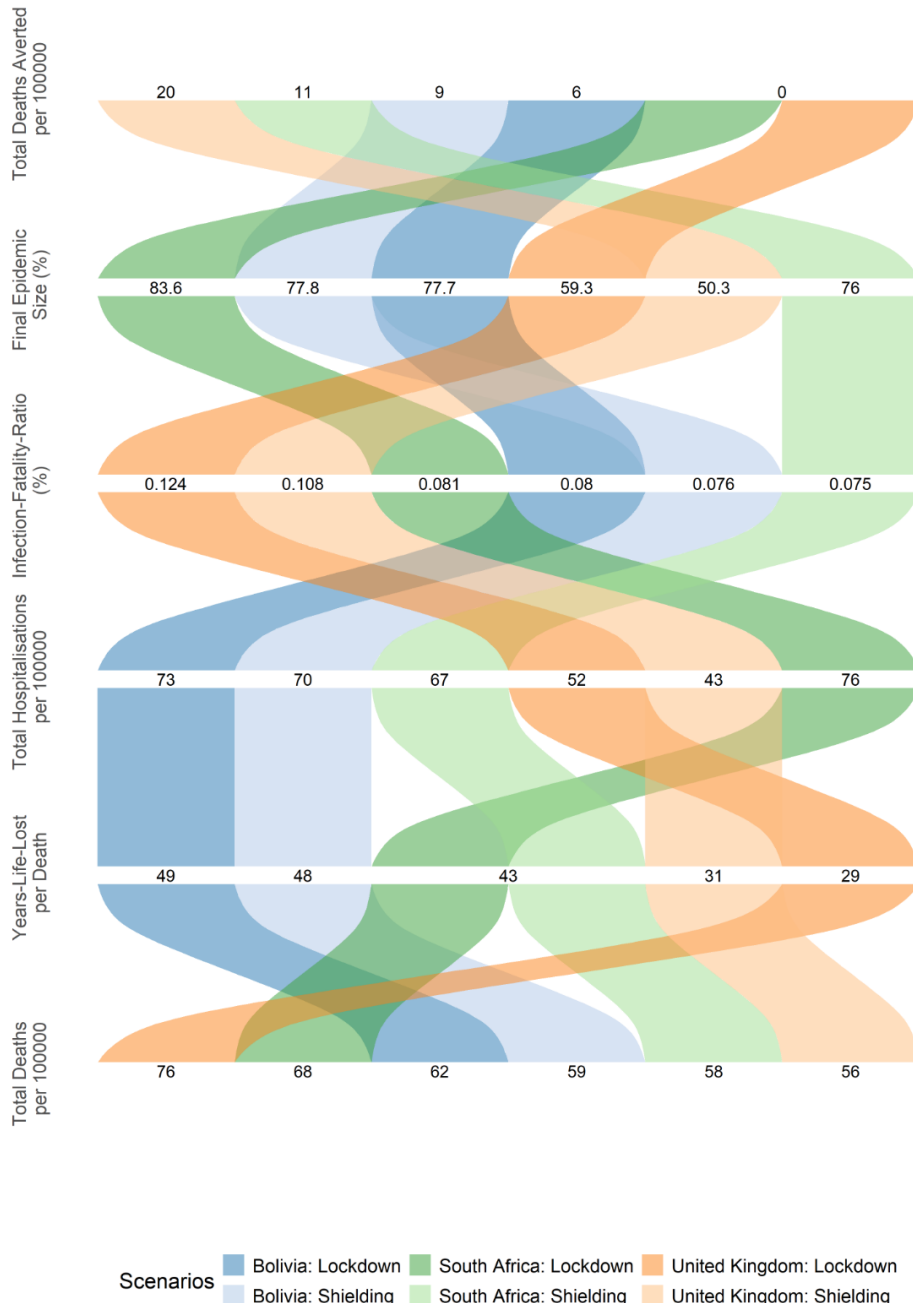


**Figure 8: Comparison of the Effectiveness of the Intervention Depending on the Outcome Metric Used: Influenza-like Outbreak** Each stream displays the outcome for a metric, averaged over the conducted runs, under the interventions (lockdown and shielding) across the three countries (Bolivia, South Africa, and the United Kingdom).

### SARS-CoV-2-like Outbreak

(Lockdown Adherence: 0.7, Shielding Adherence: 0.9, Lockdown Effective Coverage: 0.8, Shielding Effective Coverage: 0.9)

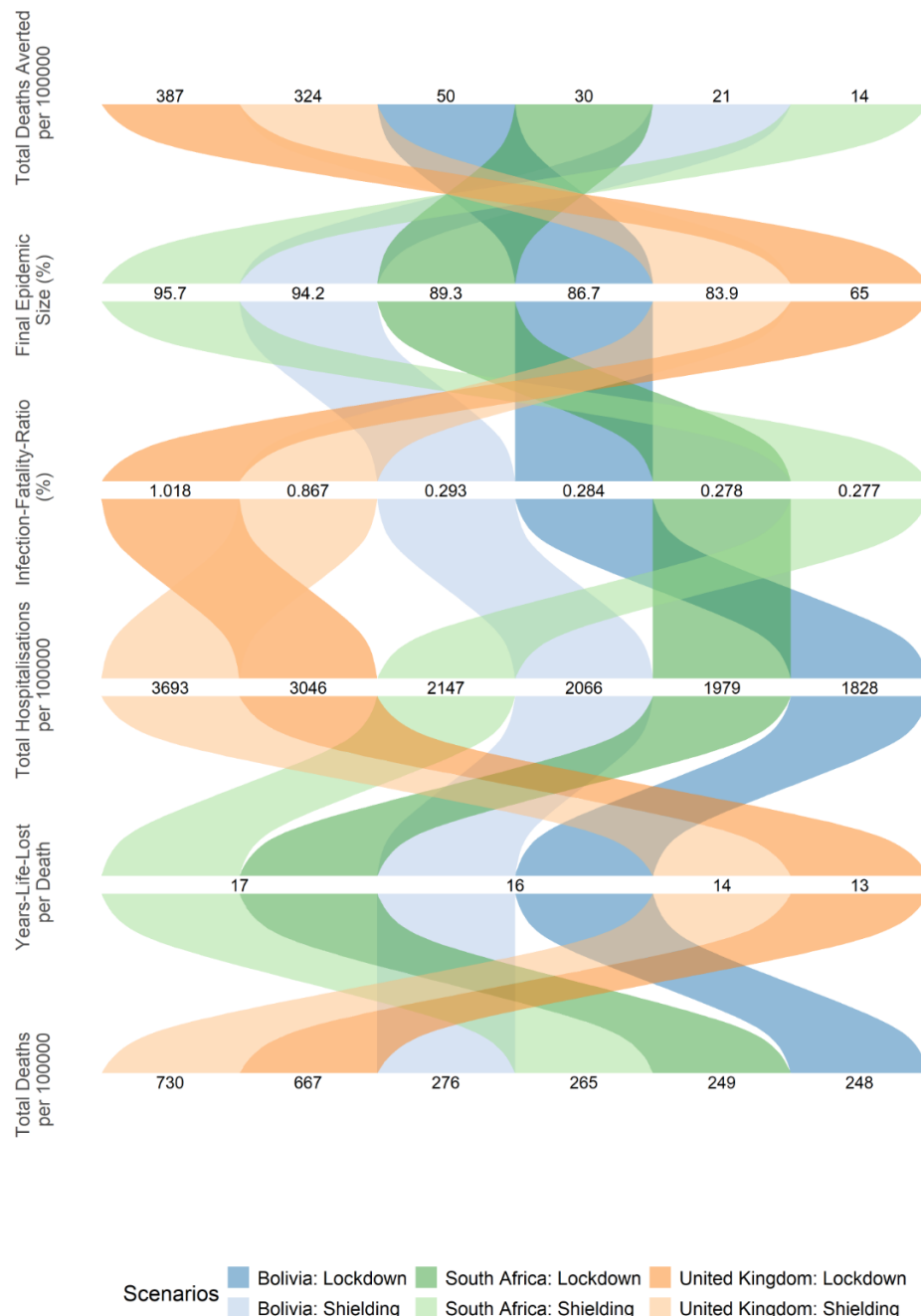


**Figure 9: Comparison of the Effectiveness of the Intervention Depending on the Outcome Metric Used: SARS-CoV-2-like Outbreak** Each stream displays the final outcome for a metric, averaged over the conducted runs, under the interventions (lockdown and shielding) across the three countries (Bolivia, South Africa, and the United Kingdom).

standard errors and 95% confidence intervals, are provided in **S3.2 Results**.

### 3.2 Impact of Virological Parameters

The boxplots - Figure 10 and 11 - consistently demonstrate that lockdowns are more effective for SARS-CoV-2-like diseases, while shielding is more beneficial for Influenza-like diseases. For Influenza-like diseases, the model shows low variability in predicted deaths across different levels of relative infectivity, indicating that this parameter has a limited impact on the effectiveness of the interventions, regardless of the strategy used. In contrast, for SARS-CoV-2-like diseases, the model's sensitivity to asymptomatic infectivity is more pronounced, highlighting that this factor heavily influences the effectiveness of interventions like lockdowns. Furthermore, for both disease types, the effectiveness of the interventions is significantly affected by variations in the probability of symptomatic infection. However, the general trend that shielding is more effective in reducing mortality for Influenza-like diseases and lockdowns for SARS-CoV-2-like diseases holds. Since the parameters have only been varied by a specific range of 30%, further analysis has been conducted to clarify the influence of virological parameters.

Bolivia, Lockdown Adherence: 0.7, Shielding Adherence: 0.9, Lockdown Efficacy: 0.8, Shielding Efficacy: 0.9

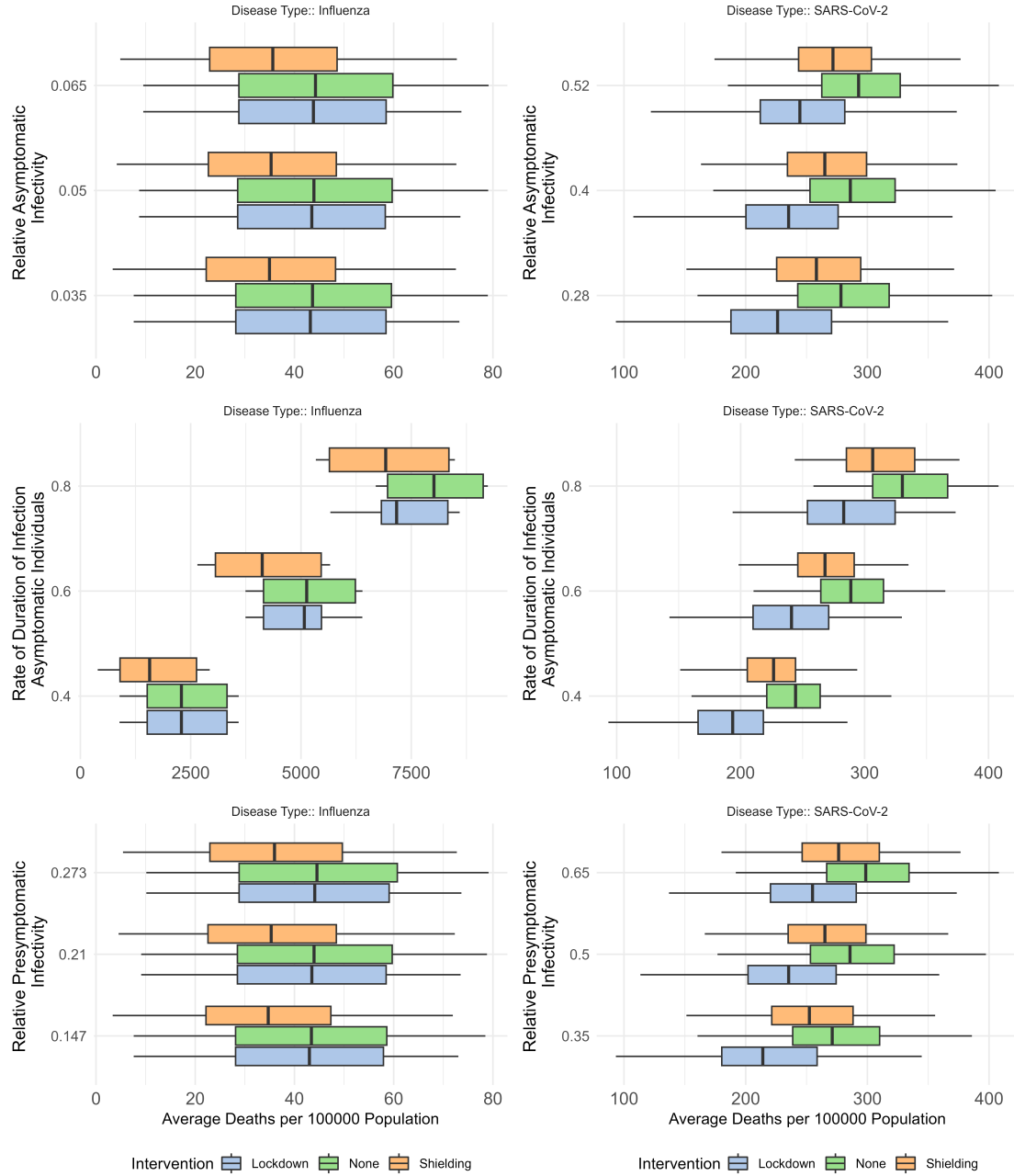


**Figure 10: Multivariate Sensitivity Analysis of the Predicted Intervention Impact on Total Deaths per 100,000 Population Depending on Disease Type** The box plots show the median and interquartile ranges of the reduction in total deaths for all simulated parameter sets. Each parameter set consists of a combination of the values depicted in 4. The simulation exclusively shows the results for the simulation scenario in Bolivia due to its proximity to the intervention's impacts. The intervention configurations have been transferred from the previous analysis setting.

The disease types can be more comprehensively explored by interchanging fundamental pre-symptomatic and asymptomatic relative infectivity values. Figure 11 shows that despite variations in relative asymptomatic infectivity, shielding consistently results in lower deaths for Influenza-like diseases, while lockdown remains the preferred strategy for SARS-CoV-2-like diseases.

Bolivia, Lockdown Adherence: 0.7, Shielding Adherence: 0.9, Lockdown Efficacy: 0.8, Shielding Efficiency: 0.9

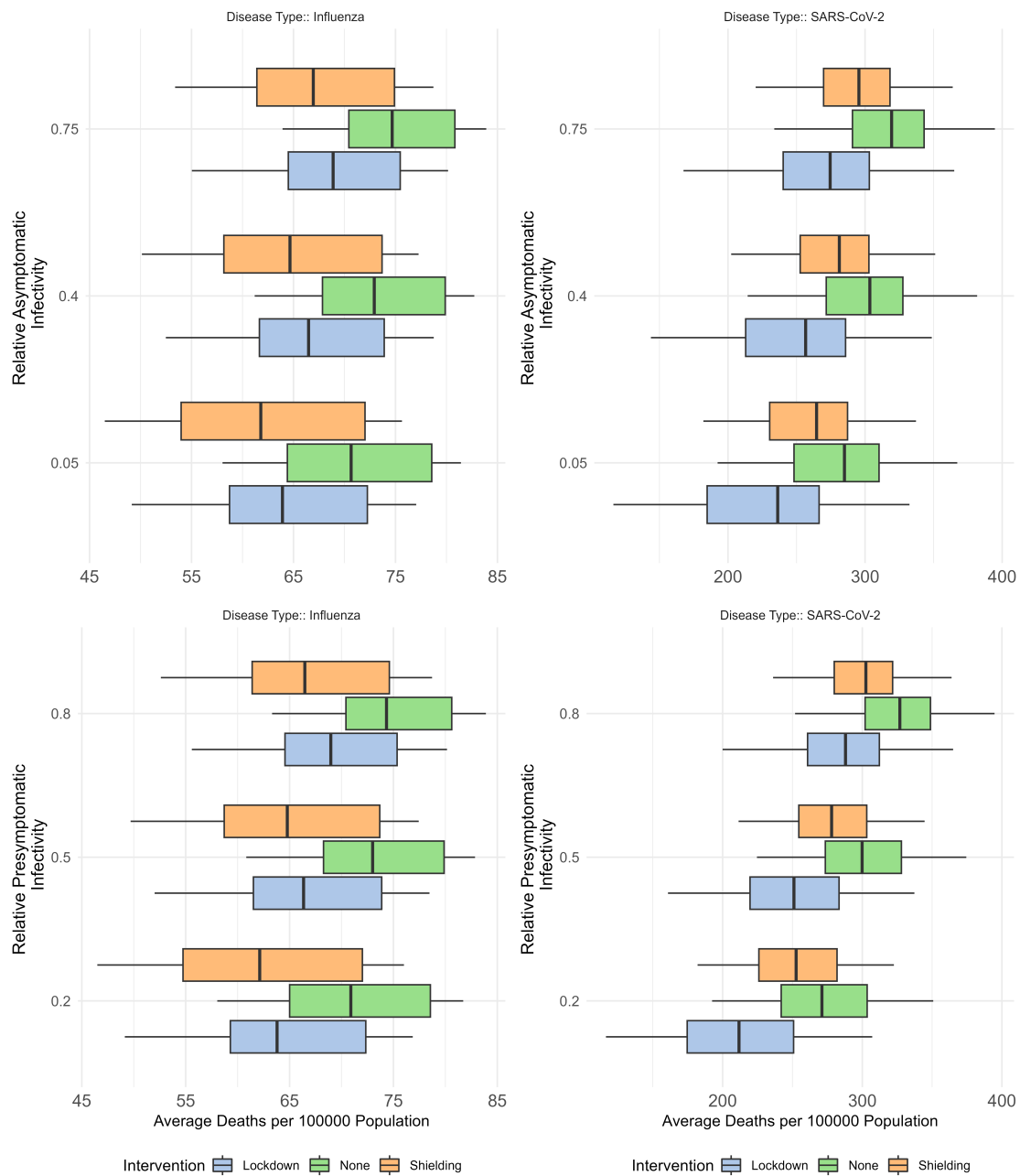


**Figure 11: Multivariate Sensitivity Analysis of the Predicted Intervention Impact on Total Deaths per 100,000 Population Depending on Disease Type Incorporating Different Relative Infectivities** The plot compares the impact of interventions across different levels of asymptomatic (top row) and presymptomatic (bottom row) infectivity for two disease types: Influenza-like (left) and SARS-CoV-2-like (right).

## 4 Discussion

We compared the impact of broad versus targeted NPIs across different diseases to identify under which demographic and immunogenic conditions one approach is superior to the other. Additionally, the study examines the virological drivers that influence these outcomes.

The results show that lockdowns lead to a more significant overall reduction in contact across the entire population. However, there are scenarios where the impact of lockdowns and shielding, in terms of decreases in outcome metrics (YLL, deaths, etc.), is comparable despite lockdowns having a clear advantage in reducing daily contacts. This measure accounts for the duration of interventions and the societal and political resources needed to sustain them. The findings reveal that shielding with higher effective coverage and adherence can achieve outcomes similar to lower-adherence lockdown strategies.

### **Interplay between Demographic and Immunogenic Traits**

Shielding is more effective in Influenza-like outbreaks, particularly in Bolivia and South Africa, where younger populations are at higher risk. This is consistent with the U-shaped age-severity curve of Influenza-like diseases, where the young and elderly are disproportionately affected. In contrast, lockdowns are more effective in SARS-CoV-2-like outbreaks, characterized by high levels of asymptomatic transmission and significant impacts on the elderly population. In all settings, shielding is less effective than lockdowns during SARS-CoV-2-like outbreaks, but the difference in total deaths between the two interventions (see **S3.4 Results**) is most pronounced in the UK, where an older population and less intergenerational mixing widen the gap.

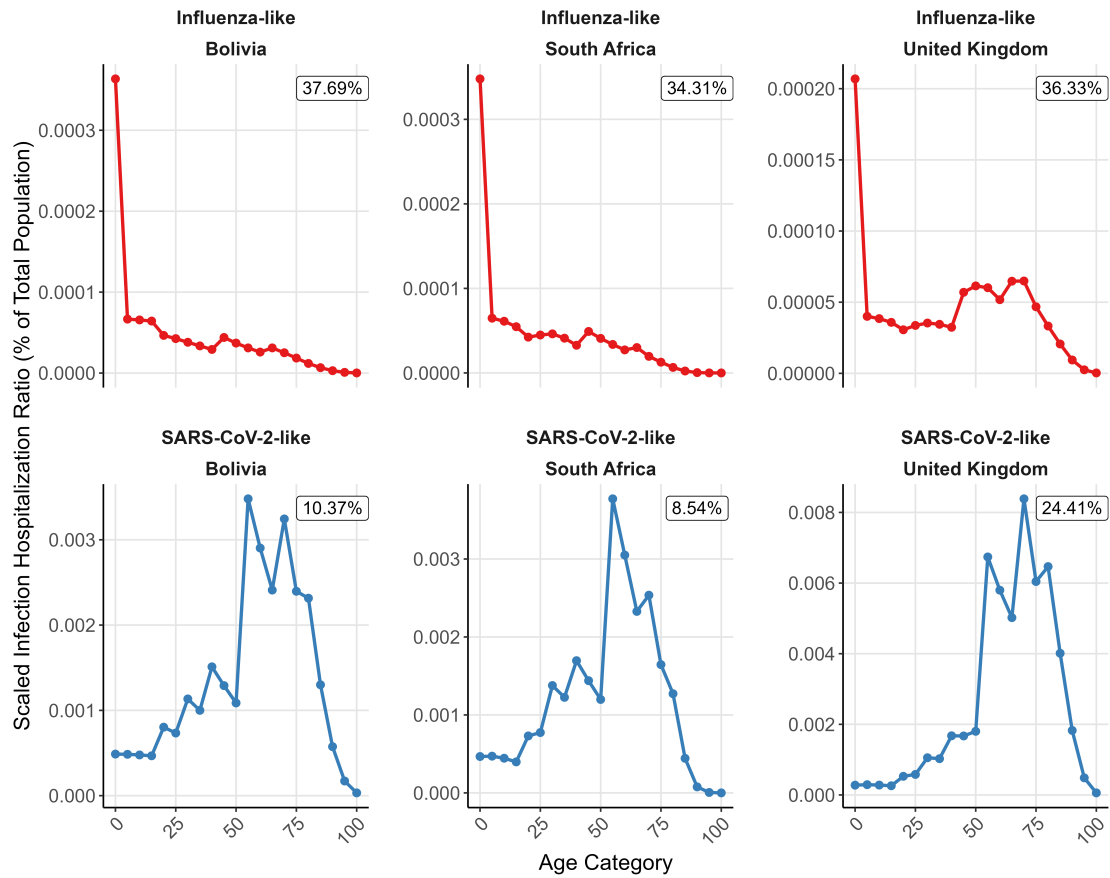


**Figure 12: Age-Stratified Infection Hospitalisation Ratio (IHR) Scaled to the Total Population for Influenza-like and SARS-CoV-2-like Illnesses Across Bolivia, South Africa, and the United Kingdom** The graphs show proportion of the entire population that is expected to be hospitalised due to infection, expressed as a percentage of the total population. The upper panels show the scaled IHR for Influenza-like illness, while the lower panels depict the scaled IHR for SARS-CoV-2-like illness. The y-axis represents the scaled IHR as a percentage of the total population. The annotations in the upper right corner of each panel indicate the population proportion in the identified risk groups (0-10 and 65+ for Influenza-like illness, 65+ for SARS-CoV-2-like illness) for each country.

The findings can be more clearly explained when considering the age-severity curve in the context of demographic structure. The scaled IHR presented in Figure 12 reflects the combined effect of age-specific hospitalisation risk and the population proportion in

each age group. In cases where the age distribution of a population closely aligns with the pathogen's age-severity curve (compare Figure 3), targeted strategies like shielding are more effective, as observed in Bolivia and South Africa during Influenza-like outbreaks. A significant proportion of the risk groups fall within the target group, enhancing the intervention's relative impact in Influenza-like outbreaks but leading to low effects during a SARS-CoV-2-like outbreak.

### **Influence of Outcome Metrics Used**

These findings hold mostly true for different outcome metrics. However, there are scenarios where, against expectations, shielding would be preferred in a SARS-CoV-2-like outbreak and vice versa, which shows that policy decisions can only be optimal for a specific outcome metric. The most apparent exceptions have been found in the metrics of YLL per death, final epidemic size and IFR.

The differences in epidemic size and total deaths in Bolivia in the SARS-CoV-2-like outbreak suggest that population structure and contact patterns play crucial roles. Bolivia's unique structure, characterized by higher intergenerational mixing, explains why shielding is less effective there than in South Africa.

### **Impact of Virological Parameters**

The sensitivity analysis confirms that lockdowns are particularly effective in scenarios where high asymptomatic infectivity drives transmission, such as in SARS-CoV-2-like diseases. However, shielding remains more resilient across varying levels of relative infectivity and proves effective in Influenza-like diseases regardless of parameter variation. These results emphasise that lockdowns are preferred in scenarios with substantial asymptomatic infectivity, shielding remains an option when high-risk groups contribute

highly as a portion of the population.

## **Limitations**

The model's calibration with data from the United Kingdom introduces potential uncertainties when applying these findings globally. Demographic structures, such as age distribution and population density, vary significantly across regions and could influence the results when generalised to other populations.

Additionally, modelling lockdown interventions is complex. Since the transmission probability directly correlates with time (and how many people can be infected), assumptions about the duration and intensity of lockdowns may not be universally applicable.

The assumptions about adherence and effective coverage generally are context-dependent, as adherence rates and enforcement levels differ across countries. While strict regulations may achieve near-perfect compliance in some settings (e.g., Singapore), the same cannot be assumed in regions with less severe penalties.

The study also does not account for reinfections or seasonality, focusing on a single year of disease spread. Future models should incorporate these factors and natural population changes to reflect more realistic dynamics over extended periods.

A part of the analysis has been conducted for a particular configuration of interventions, given explicit values for adherence and adequate coverage only in Bolivia to make them comparable. This could limit the generalisation of the finding, especially since these values are country-dependent.

Within the sensitivity analysis, it is essential to note that differences between disease types go beyond the parameters discussed, with other factors likely influencing the out-

comes. The zero values observed for the pathogen with a single-side age-severity curve and low relative infectivity suggest the outbreak may not occur, highlighting the need for more precise calibrations. The interaction between virological parameters significantly impacts  $R_0$  and the shape of the outbreak. The model's sensitivity is also evident from the high epidemic size in Influenza-like scenarios compared to the baseline, driven by variations in virological parameters.

## Future Work

Future research will expand the sensitivity analysis to explore additional demographics, interventions, and disease types. A particular focus will be on incorporating a SARS-CoV-1-like disease characterised by a non-infectious presymptomatic phase. Countries will be selected based on generalized metrics, such as age distribution, rather than specific nations, allowing for broader applicability. A systematic analysis will also explore how different virological and demographic characteristics influence intervention effectiveness.

Lockdown durations have varied significantly across countries, with literature reporting values ranging from 15 to 172 days, often averaging around 2 to 3 months depending on the nation [56–58]. Further refinement of the model will involve adjusting hospital thresholds and varying lockdown durations to capture the full spectrum of intervention impacts. The model's approach to contact matrices will also be adjusted to account for increased household mixing during lockdowns, making the comparison between shielding and lockdown more precise.

Given the model's capability to handle a wide range of demographic structures, with access to comprehensive population data for numerous countries [59, 60], the scenario

evaluation can be easily extended. As detailed in **S.1.1 Methods**, the model can dynamically calibrate disease types, providing a substantial foundation for exploring various scenarios in the future. While the study provides a framework for intervention decisions, further refinement is necessary to ensure broad generalisation.

## Conclusions

The study demonstrates that while blanket interventions like lockdowns reduce transmission more effectively on a population-wide scale, targeted strategies like shielding can achieve comparable outcomes under certain conditions. Duration and population adherence are critical factors determining intervention success. The alignment between the pathogen's age-severity curve and the population's age structure is a key determinant of targeted strategies' effectiveness. When a significant portion of the population falls within the high-risk group, targeted approaches can be more effective than blanket interventions. This effect can be amplified by low intergenerational mixing within society. This study's results have specific implications for intervention choices. The findings highlight that although asymptomatic transmission favours lockdowns, the preferred strategy ultimately depends on the chosen outcome metrics.

**Wordcount: 3987**

## hyperref Author Contributions

Conceptualization and Supervision: RA, LW

Formal Analysis: RA, BG

Methodology and Writing (Original Draft): RA

## Competing Interests

The author declares that no competing interests exist.

## Financial Disclosure

The author received no specific funding for this work.

## Data Availability

This study uses only publicly available datasets, with relevant web links provided below.

There are no restrictions on data availability. The original sources are cited at relevant points throughout the project. The datasets can be accessed as follows:

- **Case Fatality Rate (CFR) for both pathogen types:** Accessible via *Figshare*.
- **IHR for SARS-CoV-2-like diseases:** Accessible via *GitHub*.
- **Hospital beds per 10,000 population:** Accessible via *WHO Global Health Observatory*.
- **Data for the calculation of YLL:**
  - **Person-years lived above age x:** Accessible via *WHO Life Expectancy Data*.
  - **Number of people left alive at age x:** Accessible via *WHO Life Expectancy Data*.

The IHR and HFR for the Influenza-like pathogen and the HFR for the SARS-CoV-2-like pathogen have been manually transferred to Excel sheets from their respective sources, as described in the methodology. S2 Data provides a guide on accessing the data, including links to a repository.

## **Code Availability**

The code used in this paper will be submitted with this dissertation appended as a zip as well on GitHub under the following link: GitHub Repository: Dissertation Intervention Modelling. The code is further explained by additional comments made in each file. The version of R used throughout this project is 4.3.1 (R Core Team 2023) and for RStudio 2023.09.1. Packages and libraries are all named in the GitHub file *Packages and Libraries.md*.

## **Software and Code**

The version of R used throughout this project is 4.3.1 (R Core Team 2023) and for RStudio 2023.09.1. Packages and libraries are all named in the GitHub file *Packages and Libraries.md*.

# **Supplementary Information Captions**

## **S1 Methods**

**S1.1 Text - Computational Calibration of the Virological Parameters** Summary of the calibration process of the virological parameters for Influenza-like and SARS-CoV-2-like models using a custom R script. The calibration scripts and SEIR model are available in the *Calibration* folder on GitHub.

**S1.2 Text - Calculation of the Basic Reproduction Number R0** This section describes the calculation of the R0 for the pathogen types within the SEIR model.

## **S2 Data**

**S2.1 Table - R-Scripts and Data integrated into the Simulation Process** This table summarises the files used in the simulation process, detailing their purposes and any required user actions.

**S2.2 Table - Data used in the SEIR Model** This table summarises the external data sources integrated into the SEIR model via the *ModelRuns.xlsx* file. It includes descriptions, sources, and links to the corresponding files in the *Data* folder on GitHub.

## **S3 Results**

**S3.1 Text - Calculation of Integral of Effective Contact Reduction and YLL** This section explains the calculation of the two key metrics within the analysis of the results.

**S3.2 Table - Ranking of the Intervention Strategies by different Outcome Metrics** The tables present the ranking of intervention strategies based on various outcome

metrics, including total deaths per 100,000 population, YLL per death, total hospitalisations per 100,000 population, final epidemic size, infection fatality ratio, and total deaths averted per 100,000 population. The tables show mean values over simulation runs, including 95% confidence intervals and standard errors.

**S3.3 File - Results generated by the SEIR Model Simulations** This section provides hyperlinks to the results generated by the SEIR model simulations.

**S3.4 Figure - Difference in Deaths per 100,000 Population Between Lockdown and Shielding Interventions Across Bolivia, South Africa, and the United Kingdom**

## References

- [1] Jit M Edmunds WJ Fleming D Miller E Cromer D, van Hoek AJ. The burden of influenza in england by age and clinical risk group: a statistical analysis to inform vaccine policy. *J Infect*, 68(4):363–371, 2014. doi: 10.1016/j.jinf.2013.11.013. URL <https://www.sciencedirect.com/science/article/pii/S0163445313003733>.
- [2] Ocelhay O. mort\_sever\_default.rda, 2024. URL <https://github.com/ocelhay/como/tree/master/inst/comoapp/www/data>. Accessed 2024 Aug 2.
- [3] Birrell P Elgohari S Hope R Mandal S et al. Kirwan PD, Charlett A. Trends in covid-19 hospital outcomes in england before and after vaccine introduction, a cohort study. *Nat Commun*, 13(1):4834, 2022. doi: 10.1038/s41467-022-32458-y. URL <https://doi.org/10.1038/s41467-022-32458-y>.
- [4] Faivre B Sorci G. Age-dependent virulence of human pathogens. *PLoS Pathog*, 18(9):e1010866, 2022. doi: 10.1371/journal.ppat.1010866. URL <https://doi.org/10.1371/journal.ppat.1010866>.
- [5] Ghebrehewet S Koppolu V Vasigala VK Ebrahimpour S Javanian M, Barary M. A brief review of influenza virus infection. *J Med Virol*, 93(8):4638–4646, 2021. ISSN 1096-9071. doi: 10.1002/jmv.26990. URL <https://onlinelibrary.wiley.com/doi/abs/10.1002/jmv.26990>.
- [6] Xu RH Chan-Yeung M. Sars: Epidemiology. *Respirology*, 8(Suppl 1):S9–S14, 2003. doi: 10.1046/j.1440-1843.2003.00518.x. URL <https://doi.org/10.1046/j.1440-1843.2003.00518.x>.

- [7] To KK Yuen KY Cheng VC, Chan JF. Clinical management and infection control of sars: Lessons learned. *Antiviral Res*, 100(2):407–419, 2013. doi: 10.1016/j.antiviral.2013.08.016. URL <https://doi.org/10.1016/j.antiviral.2013.08.016>.
- [8] Brooks-Pollock E Edmunds WJ Eames KTD, Tilston NL. Measured dynamic social contact patterns explain the spread of h1n1v influenza. *PLoS Comput Biol*, 8, March 2012. ISSN 1553-7358. doi: 10.1371/journal.pcbi.1002425. URL <https://journals.plos.org/ploscompbiol/article?id=10.1371/journal.pcbi.1002425>.
- [9] Hupert N Shretta R Pan-Ngum W Celhay O Moldokmatova A Arifi F Mirzazadeh A Sharifi H Adib K Sahak MN Franco C Coutinho R Aguas R, White L. Modelling the covid-19 pandemic in context: an international participatory approach. *BMJ Glob Health*, 5(12):e003126, December 2020. ISSN 2059-7908. doi: 10.1136/bmjgh-2020-003126. URL <https://www.ncbi.nlm.nih.gov/pmc/articles/PMC7759758/>.
- [10] Moss PAH Glynn JR. Systematic analysis of infectious disease outcomes by age shows lowest severity in school-age children. *Sci Data*, 7:329, October 2020. ISSN 2052-4463. doi: 10.1038/s41597-020-00668-y. URL <https://www.nature.com/articles/s41597-020-00668-y>.
- [11] Faivre B Sorci G. Age-dependent virulence of human pathogens. *PLoS Pathog*, 18(9):e1010866, September 2022. ISSN 1553-7366. doi: 10.1371/journal.ppat.1010866. URL <https://www.ncbi.nlm.nih.gov/pmc/articles/PMC9531802/>.

- [12] Liu Y Prem K Jit M Pearson C Quilty B Kucharski A Gibbs H Clifford S Gimma A Zandvoort K Munday J Diamond C Edmunds W Houben R Hellewell J Russell T Abbott S Eggo R Davies N, Klepac P. Age-dependent effects in the transmission and control of covid-19 epidemics. *Nat Med*, 26:1–7, 08 2020. doi: 10.1038/s41591-020-0962-9.
- [13] Gandy A Unwin HJT Mellan TA Coupland H Whittaker C Zhu H Berah T Eaton JW Monod M Ghani AC Donnelly CA Riley S Vollmer MAC Ferguson NM Okell LC Bhatt S Flaxman S, Mishra S. Estimating the effects of non-pharmaceutical interventions on covid-19 in europe. *Nature*, 584:257–261, August 2020. ISSN 1476-4687. doi: 10.1038/s41586-020-2405-7. URL <https://www.nature.com/articles/s41586-020-2405-7>.
- [14] Bram A. D. van Bunnik, Alex L. K. Morgan, Paul R. Bessell, Giles Calder-Gerver, Feifei Zhang, and Samuel Haynes. Immunological characteristics of covid-19 and the impact of age. *Philosophical Transactions of the Royal Society B: Biological Sciences*, 376:20200275, 2021. doi: 10.1098/rstb.2020.0275. URL <https://royalsocietypublishing.org/doi/full/10.1098/rstb.2020.0275>.
- [15] Gandy A et al. Flaxman S, Mishra S. Estimating the effects of non-pharmaceutical interventions on covid-19 in europe. *Nature*, 584:257–261, 2020. doi: 10.1038/s41586-020-2405-7.
- [16] Maria C. Zambon. Epidemiology and pathogenesis of influenza. *Journal of Antimicrobial Chemotherapy*, 44(suppl\_2):3–9, November 1999. doi: 10.1093/jac/44.suppl\_2.3. URL [https://doi.org/10.1093/jac/44.suppl\\_2.3](https://doi.org/10.1093/jac/44.suppl_2.3).
- [17] Kiesha Prem, Alex R. Cook, and Mark Jit. Projecting social contact matrices in

- 152 countries using contact surveys and demographic data. *PLOS Computational Biology*, 13(9):1–21, 2017. doi: 10.1371/journal.pcbi.1005697. URL <https://doi.org/10.1371/journal.pcbi.1005697>.
- [18] Worldometer. United kingdom covid-19 statistics, 2024. URL <https://www.worldometers.info/coronavirus/country/uk/#graph-deaths-daily>. Accessed 2024 Aug 3.
- [19] World Health Organization. Hospital beds (per 10 000 population), 2023. URL [https://www.who.int/data/gho/data/indicators/indicator-details/GHO/hospital-beds-\(per-10-000-population\)](https://www.who.int/data/gho/data/indicators/indicator-details/GHO/hospital-beds-(per-10-000-population)). Accessed 2024 Aug 2.
- [20] Moyes J McMorrow ML Treurnicht FK Hellferssee O et al. Cohen C, Kleynhans J. Asymptomatic transmission and high community burden of seasonal influenza in an urban and a rural community in south africa, 2017-18 (phirst): a population cohort study. *Lancet Glob Health*, 9(6):e863–e874, 2021. doi: 10.1016/S2214-109X(21)00141-8.
- [21] Mermel LA Patrozou E. Does influenza transmission occur from asymptomatic infection or prior to symptom onset? *Public Health Rep*, 124(2):193–196, 2009. doi: 10.1177/003335490912400205.
- [22] Ip DKM Cowling BJ Leung NHL, Xu C. The fraction of influenza virus infections that are asymptomatic. *Epidemiology*, 26(6):862–872, 2015. doi: 10.1097/EDE.0000000000000340.
- [23] Fang VJ Chan KH Lau EHY Lipsitch M et al. Lau LLH, Cowling BJ. Viral shedding and clinical illness in naturally acquired influenza virus infections. *J Infect Dis*, 201(10):1509–1516, 2010. doi: 10.1086/652241.

- [24] J. He, Y. Guo, R. Mao, and J. Zhang. Proportion of asymptomatic coronavirus disease 2019: A systematic review and meta-analysis. *Journal of Medical Virology*, 93(2):820–830, 2021. doi: 10.1002/jmv.26326. URL <https://doi.org/10.1002/jmv.26326>.
- [25] M. Alene, L. Yismaw, M. A. Assemie, D. B. Ketema, B. Mengist, B. Kassie, et al. Magnitude of asymptomatic covid-19 cases throughout the course of infection: A systematic review and meta-analysis. *PLOS ONE*, 16(3):e0249090, 2021. doi: 10.1371/journal.pone.0249090. URL <https://doi.org/10.1371/journal.pone.0249090>.
- [26] D. P. Oran and E. J. Topol. The proportion of sars-cov-2 infections that are asymptomatic: A systematic review. *Annals of Internal Medicine*, 174(5):682–692, 2021. doi: 10.7326/M20-6976. URL <https://doi.org/10.7326/M20-6976>.
- [27] B. Wang, P. Andraweera, S. Elliott, H. Mohammed, Z. Lassi, A. Twigger, et al. Asymptomatic sars-cov-2 infection by age: A global systematic review and meta-analysis. *The Pediatric Infectious Disease Journal*, 42(3):232–239, 2023. doi: 10.1097/INF.0000000000003791. URL <https://doi.org/10.1097/INF.0000000000003791>.
- [28] Centers for Disease Control and Prevention. How flu spreads, 2024. URL <https://www.cdc.gov/flu/about/disease/spread.htm>. Accessed: 2024-07-30.
- [29] Centers for Disease Control and Prevention. Key facts about seasonal flu, 2024. URL <https://www.cdc.gov/flu/about/keyfacts.htm>. Accessed: 2024-07-30.
- [30] Schink SB Schweiger B Heider A Milde J et al. Suess T, Remschmidt C. Com-

- parison of shedding characteristics of seasonal influenza virus (sub)types and influenza a(h1n1)pdm09; germany, 2007–2011. *PLoS One*, 7(12):e51653, 2012. doi: 10.1371/journal.pone.0051653.
- [31] Hupert N Shretta R Pan-Ngum W Celhay O Moldokmatova A Arifi F Mirza-zadeh A Sharifi H Adib K Sahak MN Franco C Coutinho R CoMo Consortium Aguas R, White L. Modelling the covid-19 pandemic in context: An international participatory approach. *BMJ Glob Health*, 5(12):e003126, 2020. doi: 10.1136/bmjgh-2020-003126. URL <https://doi.org/10.1136/bmjgh-2020-003126>.
- [32] Ocelhay V. Template\_comocovid-19app\_v17.xlsx file from como repository, 2023. URL [https://github.com/ocelhay/como/blob/master/Template\\_CoMoCOVID-19App\\_v17.xlsx](https://github.com/ocelhay/como/blob/master/Template_CoMoCOVID-19App_v17.xlsx). Accessed: 2024-08-13.
- [33] CoMo Consortium. Como model, 2024. URL <https://comomodel.net/>. Accessed: 2024-08-13.
- [34] Moyes J McMorrow ML Treurnicht FK Hellferscee O et al. Cohen C, Kleyn-hans J. Asymptomatic transmission and high community burden of seasonal influenza in an urban and a rural community in south africa, 2017-18 (phirst): a population cohort study. *Lancet Glob Health*, 9(6):e863–e874, 2021. doi: 10.1016/S2214-109X(21)00141-8. URL [https://doi.org/10.1016/S2214-109X\(21\)00141-8](https://doi.org/10.1016/S2214-109X(21)00141-8).
- [35] Wang C et al. Cao S, Gan Y. Post-lockdown sars-cov-2 nucleic acid screening in nearly ten million residents of wuhan, china. *Nat Commun*, 11:5917, 2020. doi: 10.1038/s41467-020-19802-w.
- [36] Cervellati C Rizzo R Zuliani G Zuin M, Gentili V. Viral load difference between

- symptomatic and asymptomatic covid-19 patients: Systematic review and meta-analysis. *Infect Dis Rep*, 13(3):645–653, 2021. doi: 10.3390/idr13030061.
- [37] Asilturk D et al. Hasanoglu I, Korukluoglu G. Higher viral loads in asymptomatic covid-19 patients might be the invisible part of the iceberg. *Infection*, 49:117–126, 2021. doi: 10.1007/s15010-020-01548-8.
- [38] World Health Organization. Influenza (seasonal). [https://www.who.int/news-room/fact-sheets/detail/influenza-\(seasonal\)](https://www.who.int/news-room/fact-sheets/detail/influenza-(seasonal)), 2023. Accessed: 2024-08-26.
- [39] World Health Organization. Influenza (seasonal), 2024. URL [https://www.who.int/news-room/fact-sheets/detail/influenza-\(seasonal\)](https://www.who.int/news-room/fact-sheets/detail/influenza-(seasonal)). Accessed: 2024-07-30.
- [40] Hui DSC Rainer TH Wong E Choi KW et al. Lee N, Chan PKS. Viral loads and duration of viral shedding in adult patients hospitalized with influenza. *J Infect Dis*, 200(4):492–500, 2009. doi: 10.1086/600383.
- [41] Uribe-Noguez LA et al. Santos Coy-Arechavaleta A, Alvarado-Yaah JE. Relationship between the viral load in patients with different covid-19 severities and sars-cov-2 variants. *Microorganisms*, 12(3):428, 2024. doi: 10.3390/microorganisms12030428.
- [42] Schink SB Schweiger B-Heider A Milde J et al. Suess T, Remschmidt C. Comparison of shedding characteristics of seasonal influenza virus (sub)types and influenza a(h1n1)pdm09; germany, 2007–2011. *PLoS ONE*, 7(12):e51653, 2012. doi: 10.1371/journal.pone.0051653. URL <https://doi.org/10.1371/journal.pone.0051653>.

- [43] Centers for Disease Control and Prevention. Key facts about influenza (flu), 2024. URL <https://www.cdc.gov/flu/about/keyfacts.htm>. Accessed 2024 Jul 30.
- [44] Centers for Disease Control and Prevention. Covid-19, 2024. URL <https://wwwnc.cdc.gov/travel/yellowbook/2024/infections-diseases/covid-19>. Accessed 2024 Jul 30.
- [45] National Health Service. How to avoid catching and spreading covid-19, 2024. URL <https://www.nhs.uk/conditions/covid-19/how-to-avoid-catching-and-spreading-covid-19/>. Accessed 2024 Jul 30.
- [46] Reed C Gambhir M-Finelli L Biggerstaff M, Cauchemez S. Estimates of the reproduction number for seasonal, pandemic, and zoonotic influenza: a systematic review of the literature. *BMC Infect Dis*, 14:480, 2014. doi: 10.1186/1471-2334-14-480. URL <https://doi.org/10.1186/1471-2334-14-480>.
- [47] Virginia Department of Health. Covid-19 and influenza surveillance, 2022. URL <https://www.vdh.virginia.gov/coronavirus/2022/01/07/covid-19-and-influenza-surveillance/>. Accessed 2024 Jul 30.
- [48] Virginia Department of Health. Covid-19 and influenza surveillance. <https://www.vdh.virginia.gov/coronavirus/2022/01/07/covid-19-and-influenza-surveillance/#:~:text=For%20the%20flu%20the%20R0,flu%2C%20between%202%20and%203.,> 2022. Accessed: 2024-07-30.
- [49] Wang MH et al. Musa SS, Zhao S. Estimation of exponential growth rate and basic

- reproduction number of the coronavirus disease 2019 (covid-19) in africa. *Infect Dis Poverty*, 9:96, 2020. doi: 10.1186/s40249-020-00718-y.
- [50] Rousson V Locatelli I, Trächsel B. Estimating the basic reproduction number for covid-19 in western europe. *PLoS One*, 16(3):e0248731, 2021. doi: 10.1371/journal.pone.0248731.
- [51] European Centre for Disease Prevention and Control. Seasonal influenza, 2024. URL <https://www.ecdc.europa.eu/en/seasonal-influenza>. Accessed 2024 Jul 30.
- [52] Jenks S et al. Brazeau NF, Verity R. Estimating the covid-19 infection fatality ratio accounting for seroreversion using statistical modelling. *Commun Med*, 2: 54, 2022. doi: 10.1038/s43856-022-00106-7.
- [53] World Health Organization. Influenza (seasonal), 2023. URL [https://www.who.int/news-room/fact-sheets/detail/influenza-\(seasonal\)](https://www.who.int/news-room/fact-sheets/detail/influenza-(seasonal)). Accessed: 2024-08-19.
- [54] A. L. Lloyd. Sensitivity of model-based epidemiological parameter estimation to model assumptions. In *Mathematical and Statistical Estimation Approaches in Epidemiology*, pages 123–141. Springer, 2009. doi: 10.1007/978-90-481-2313-1-6.
- [55] Nikolaou M. Revisiting the standard for modeling the spread of infectious diseases. *Sci Rep*, 12(7077), 2022. doi: 10.1038/s41598-022-10185-0. URL <https://doi.org/10.1038/s41598-022-10185-0>.
- [56] J. Pavani, J. Cerdá, L. Gutiérrez, et al. Factors associated to the duration of covid-19 lockdowns in chile. *Scientific Reports*, 12:9516,

2022. doi: 10.1038/s41598-022-13743-8. URL <https://doi.org/10.1038/s41598-022-13743-8>.
- [57] Mario Coccia. The relation between length of lockdown, numbers of infected people and deaths of covid-19, and economic growth of countries: Lessons learned to cope with future pandemics similar to covid-19 and to constrain the deterioration of economic system. *Science of The Total Environment*, 775:145801, 2021. ISSN 0048-9697. doi: <https://doi.org/10.1016/j.scitotenv.2021.145801>. URL <https://www.sciencedirect.com/science/article/pii/S0048969721008688>.
- [58] Daniel Griffiths, Luke Sheehan, Dennis Petrie, Caryn van Vreden, Peter Whiteford, and Alex Collie. The health impacts of a 4-month long community-wide covid-19 lockdown: Findings from a prospective longitudinal study in the state of victoria, australia. *PLOS ONE*, 17(4):e0266650, April 2022. doi: 10.1371/journal.pone.0266650. URL <https://doi.org/10.1371/journal.pone.0266650>.
- [59] United Nations, Department of Economic and Social Affairs, Population Division. World population prospects: The 2022 revision, 2022. URL <https://population.un.org/wpp/Download/Standard/Population/>. Accessed: 2024-08-13.
- [60] Ocelhay V. demog.rda file from como repository, 2023. URL <https://github.com/ocelhay/como/blob/master/inst/comoapp/www/data/demog.Rda>. Accessed: 2024-08-13.
- [61] Z. Karimizadeh, R. Dowran, T. Mokhtari-Azad, et al. The reproduction rate of severe acute respiratory syndrome coronavirus 2 different variants recently circulated in humans: A narrative review. *European Journal of Medical Research*, 28

- (94), 2023. doi: 10.1186/s40001-023-01047-0. URL <https://doi.org/10.1186/s40001-023-01047-0>.
- [62] Schink SB Schweiger B-Heider A Milde J et al. Suess T, Remschmidt C. Comparison of shedding characteristics of seasonal influenza virus (sub)types and influenza a(h1n1)pdm09; germany, 2007–2011. *PLoS ONE*, 7(12):e51653, 2012. doi: 10.1371/journal.pone.0051653. URL <https://doi.org/10.1371/journal.pone.0051653>.
- [63] Maria C. Zambon. Epidemiology and pathogenesis of influenza. *J Antimicrob Chemother*, 44(suppl 2):3–9, Nov 1999. ISSN 0305-7453. doi: 10.1093/jac/44.suppl\_2.3. URL [https://doi.org/10.1093/jac/44.suppl\\_2.3](https://doi.org/10.1093/jac/44.suppl_2.3).
- [64] Schain M Mansour Y. Learning with maximum-entropy distributions. *Mach Learn*, 45(2):123–145, 2001. doi: 10.1023/A:1010950718922. URL <https://doi.org/10.1023/A:1010950718922>.
- [65] Zhu Z Thomas DR, Yeung P. *Proximity: Calculate proximity measures between categorical data in stepwiseCM: Variable selection and classification in categorical data*, 2024. Available from: <https://www.rdocumentation.org/packages/stepwiseCM/versions/1.18.0/topics/Proximity>.
- [66] Ocelhay V. contacts.rda file from como repository, 2023. URL <https://github.com/ocelhay/como/blob/master/inst/comoapp/www/data/contacts.Rda>. Accessed: 2024-08-13.
- [67] World Health Organization. number of people left alive at age x, 2024. URL [https://apps.who.int/gho/data/node.imr.LIFE\\_0000000031?lang=en](https://apps.who.int/gho/data/node.imr.LIFE_0000000031?lang=en). Accessed: 2024-08-30.

[68] World Health Organization. person-years lived above age x, 2024. URL [https://apps.who.int/gho/data/node.imr.LIFE\\_000000034?lang=en](https://apps.who.int/gho/data/node.imr.LIFE_000000034?lang=en). Accessed: 2024-08-30.

## **Supplementary Materials**

# **S1 Methods**

## **Contents**

**S1.1 Text** - Computational Calibration of the Virological Parameters

**S1.2 Text** - Calculation of the Basic Reproduction Number R<sub>0</sub>

## S1.1 Computational Calibration of the Virological Parameters

The different disease types have been aligned with the literature to match the general characteristics of Influenza and SARS-CoV-2. After determining the ranges for all virological parameters, we generated an R-Script (File: PreAutomatic.R), which reads in ranges for all the possible parameters as a vector and creates a grid for all the possible combinations. The estimated ranges for these values are from the literature (Table 5).

**Table 5: Ranges for the Virological Parameters Used in the SEIR Modelled for Both Disease Types**

Virological Parameter	Disease A Influenza-like	Literature	Disease B SARS-CoV-like	Literature
p	/	estimated from $R_0$	0-0.2	estimated from $R_0$
$\gamma$	1/1 - 1/4	[38, 39]	1/1 - 1/7	[31]
$p_c$	0.5 - 0.96	[20–23]	0.52 - 0.85	[24–27, 61]
$\rho$	0.01 - 0.25	[28–30]	0.5	[35–37]
$v_c$	1/5 - 1/7	[43]	1/5 - 1/10	[44, 45]
$\rho_h$	1.1 - 1.3	[28]	0.6 - 0.8	[41]
$v_h$	1/5 - 1/10	[28, 40]	0.11	[41]
$\rho_a$	0.01 - 0.1	[34, 62]	0.6 - 1.1	[35–37]
$v_a$	1/4 - 1/6	[42]	1/5 - 1/10	[44, 45]
$R_0$	1.0 - 2.0	[46, 47]	2.0 - 3.0	[48–50]
IFR	~0.1%	[51]	~1%	[52]

The model was executed for all the runs (File: Sim.R). Based on these results, we estimated the best fit for the parameters matching the desired outcome values of the primary reproduction number  $R_0$  (the resulting Herd Immunity Threshold), the Infection Fatality Ratio, and the Final Epidemic Size (File: PosCalibration.R). The Random Forest algorithm calculates the proximity of every parameter set, generating a result value between 0 and 1 where 1 indicates a perfect match [64, 65]. The script generated a fitting set of virological parameters for each desired disease, matching the result characteristics.

This script can easily be used in the future to calibrate other pathogens. The files are in the *Calibartion* folder on GitHub. This folder includes a standalone file for the SEIR model (File: StandaloneNoIntervention.R), allowing for single simulation runs.

## S1.2 Calculation of the Basic Reproduction Number $R_0$

We estimated the basic reproduction number  $R_0$  as an essential calibration point for the explored pathogens. This value gives the average number of newly infected people caused by one case in a completely susceptible population. For an SIR model the estimation is the following [55]:

$$R_{0,SIR} = \frac{\ln(2) \cdot D}{T_D} + 1 \quad (14)$$

$T_d$  being the doubling time and  $D$  the duration of the infectious period. These concepts can be applied to the structure of an SEIR model according to [54]:

$$R_{0,SEIR} = (1 + r \cdot D_I) \cdot (1 + r \cdot D_E) \quad (15)$$

Combining both approaches, the following formula can be estimated:

$$R_{0,SEIR} = \left(1 + \frac{\ln(2)}{T_D} \cdot D_I\right) \cdot \left(1 + \frac{\ln(2)}{T_D} \cdot D_E\right) \quad (16)$$

, with

$$r = \frac{\ln(2)}{T_d}. \quad (17)$$

, where

$$T_d = \ln(2) \cdot D_I \cdot \frac{\ln(\text{incidence}[t=3])}{\ln(\text{incidence}[t=3 + D_I])} \quad (18)$$

$D_I$  being the weighted duration of the infectious period and  $D_E$  the duration of the latent period.

$$D_E = \frac{1}{\gamma} \quad (19)$$

$$D_I = D_C + D_H + D_A \quad (20)$$

, with the duration being for the different infectious compartments:

$$D_C = \left[ \left( \frac{1}{\gamma} \cdot \rho \right) \cdot \left( \frac{1}{v_C} \right) \right] \cdot pc \cdot (1 - IHR) \quad (21)$$

$$D_H = \left[ \left( \frac{1}{\gamma} \cdot \rho \right) \cdot \left( \frac{1}{v_H} \cdot \rho_h \right) \right] \cdot IHR \quad (22)$$

$$D_A = \left[ \left( \frac{1}{\gamma} \cdot \rho \right) \cdot \left( \frac{1}{v_A} \cdot \rho_A \right) \right] \cdot (1 - pc) \cdot (1 - IHR) \quad (23)$$

Since the infection-hospitalisation ratio is a vector, the mean of the result for  $T_d$  is taken. The durations are weighted firstly by the proportion in that compartment and secondly

by the relative infectivity compared to the C-compartment, which we considered to have infectivity 1.

## **S2 Data**

### **Contents**

**S2.1 Table** - R-Scripts and Data integrated into the Simulation Process

**S2.2 Table** - Data used in the SEIR Model

## S2.1 - R-Scripts and Data integrated into the Simulation Process

**Table 6: Summary of Files for Reproducing the Simulations Conducted Within the Study** The table lists all the files needed to execute simulations, with their respective purposes described. All files which have been used to create plots externally from the simulation process (Figure 2, 12, 13, ) can be found in the GitHub in the folder Post\_Methodology.

File Name	Description	Data Source	User Action
<b>Pre-Processing</b>			
Pre.R	Generates master file for simulations	/	Set Working Directory
DiseaseParams.xlsx	Contains all the baseline scenarios for the virological parameters for the disease types	Table 4	None
<b>Simulation</b>			
Sim.R	SEIR-Model	/	Set Working Directory and define name of master file
contacts.Rda	Contact matrices	[17, 66]	None
ModelRuns.xlsx	Combines all the necessary data needed for the simulation to execute and serves as a base for the master file	Table 7	None
<b>Post-Processing</b>			
LinePlot.R	Creates Figure 4, 5 and 6	/	Set working directory and define name of results file
Scatter.R	Creates figure 7	/	Set working directory and define name of results file
AlluvialCaseStudy.R	Creates Figure 9, 8 and 14	/	Set working directory and define name of results file
BoxplotOneCountry.R	Creates Figure 10	/	Set working directory and define name of results file

## S2.2 - Data used in the SEIR Model

**Table 7: Summary of External Data Sources for SEIR Model** The table lists the external data with their respective source, integrated into the file ModelRuns.xlsx, which provides the base information for the master file.

Sheet Name in ModelRuns.xlsx	Description	Original Source	File name in GitHub in folder <i>Data</i>
SARS-CoV-2	IHR, CFR, and HFR for SARS-CoV-2-like disease types. Shielding vector establishing the age groups.	IHR: [2] CFR: [4] HFR: [3]	CFR_Calculation.xlsx IHR_Covid.Rda
Influenza	IHR, CFR, and HFR for Influenza-like disease types. Shielding vector establishing the age groups.	IHR: [1] CFR: [4] HFR: [1]	CFR_Calculation.xlsx HFR_IHR_Influenza.xlsx
lifeexpec	Life Tables for calculating YLL	[67, 68]	LifeTablesBO.xlsx LifeTablesSA.xlsx LifeTablesUK.txt
population	Population-Age Structures of Countries	[59, 60]	N/A
hospitalbeds	Available Hospital Beds per 10,000 Population	[19]	Hospitalbeds.xlsx

## **S3 Results**

### **Contents**

**S3.1 Text** - Calculation of Integral of Effective Contact Reduction and YLL

**S3.2 Table** - Ranking of the Intervention Strategies by different Outcome Metrics

**S3.3 Data** - Results generated by the SEIR model Simulations

**S3.4 Figure** - Difference in Deaths per 100,000 Population Between Lockdown and Shielding Interventions Across Bolivia, South Africa, and the United Kingdom

### **S3.1 - Calculation of Integral of Effective Contact Reduction and YLL**

The following describes the calculation of the outcome metrics: **Integral of Effective Contact Reduction (ICER)** and **YLL**.

#### **Integral of Effective Contact Reduction**

This metric expresses the reduction in transmission potential for both targeted and blanket strategies. While blanket strategies may achieve a greater absolute reduction in contacts, they often require significantly more economic and societal resources. This value makes these two intervention strategies more comparable by accounting for their different durations since lockdown is transient and shielding is active throughout the analysis period.

For the lockdown strategy, each activation triggers a lockdown lasting 90 days, with the option to reactivate if hospitalisation rates exceed a predefined threshold. In contrast, the shielding strategy is triggered by a specific prevalence level and remains in effect until the final day of the outbreak. To ensure a fair comparison, the SEIR model filters the dates when daily prevalence drops below the threshold and considers this period the time contributing to the shielding outcome measure. Figure 13 illustrates an example of an outbreak with these interventions in place.

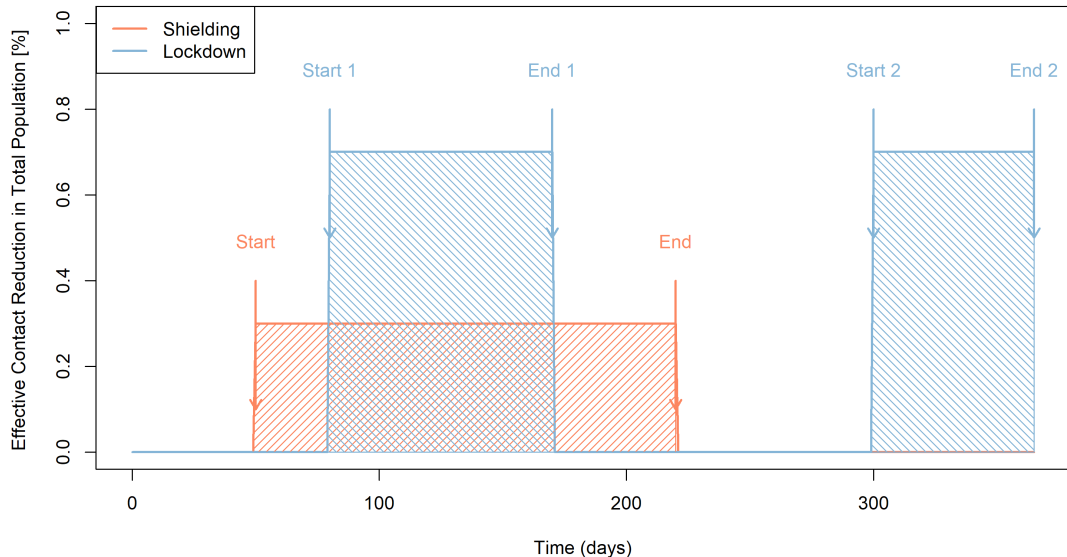


**Figure 13: Comparison of Effective Contact Reduction Over Time for Shielding and Lockdown Interventions** The plot illustrates both interventions’ start and end points, showing the percentage reduction in effective contacts within the total population. The integral as a measure is shown in the hatched areas. As depicted, the calculation accounts for lockdowns that start later than 90 days before the end of the simulation time frame by adjusting the total period.

For example, consider an IECR value of 60 for the shielding intervention in Bolivia during an influenza outbreak. This value indicates that the cumulative reduction in contacts over the intervention period is equivalent to a 60% reduction for a single day or a 20% reduction sustained over three days. The IECR, therefore, captures both the effectiveness and duration of the intervention, providing a more comprehensive view of its impact.

The IECR for run  $i$  is defined as:

$$\text{IECR}_i = \int_0^{365} \text{switch}(t) \cdot (\text{Eff}_x \times \text{Cov}_x \times \text{Adh}_x) dt \quad (24)$$

$\text{Eff}_x$  represents the efficacy of the intervention in reducing contacts,  $\text{Cov}_x$  stands for the coverage, meaning the proportion of the target population participating in the intervention, and  $\text{Adh}_x$  reflects adherence to the intervention's protocol. The  $\text{switch}(t)$  function determines whether the intervention is active (with a value of 1) or inactive (with a value of 0) at any given time.

## YLL

The YLL have been calculated using data from the life tables obtained from the World Health Organisation (WHO) [67, 68]. The result provides a vector with values in years per age group, indicating the YLL by a person dying in that age group. The value per age group is the ratio of  $T_a$ , which represents person-years lived above age  $a$ , and  $l_a$ , the number of people left alive at age  $a$  :

$$\text{expectancy}_a = \frac{T_a}{l_a} \quad (25)$$

The product of the expectancy at year  $x$  and the deaths per age group per simulation run are calculated, and the sum over all age groups provides the resulting total value of YLL

for run i:

$$YLL = \sum_a (\text{expectancy}_{a_i} \cdot \text{deaths}_{a_i}) \quad (26)$$

### S3.2 - Ranking of the Intervention Strategies by different outcome metrics

**Table 8: Intervention Strategies ranked by Total Deaths per 100,000 Population** The result depicts the mean value over the simulation runs conducted with 95% confidence interval (CI) and standard error.

Country	Disease-like Type	Intervention	Total Deaths	SE	95% CI
United Kingdom	Influenza	Shielding	56	4.59	(47, 65)
South Africa	Influenza	Shielding	58	2.12	(54, 62)
Bolivia	Influenza	Shielding	59	1.95	(55, 63)
Bolivia	Influenza	Lockdown	62	1.51	(59, 65)
South Africa	Influenza	Lockdown	68	1.58	(65, 71)
United Kingdom	Influenza	Lockdown	76	5.45	(65, 87)
Bolivia	SARS-CoV-2	Lockdown	248	6.53	(235, 261)
South Africa	SARS-CoV-2	Lockdown	249	4.99	(239, 259)
South Africa	SARS-CoV-2	Shielding	265	3.84	(257, 273)
Bolivia	SARS-CoV-2	Shielding	276	5.01	(266, 286)
United Kingdom	SARS-CoV-2	Lockdown	667	26.58	(615, 719)
United Kingdom	SARS-CoV-2	Shielding	730	17.29	(696, 764)

**Table 9: Intervention Strategies ranked by YLL per Death** The result depicts the mean value over the simulation runs conducted with 95% CI and standard error.

Country	Disease-like Type	Intervention	Average YLL Per Death	SE	95% CI
United Kingdom	SARS-CoV-2	Lockdown	13	0.05	(13, 13)
United Kingdom	SARS-CoV-2	Shielding	14	0.06	(14, 14)
Bolivia	SARS-CoV-2	Lockdown	16	0.10	(16, 16)
Bolivia	SARS-CoV-2	Shielding	16	0.10	(16, 16)
South Africa	SARS-CoV-2	Lockdown	17	0.06	(17, 17)
South Africa	SARS-CoV-2	Shielding	17	0.07	(17, 17)
United Kingdom	Influenza	Lockdown	29	0.20	(29, 29)
United Kingdom	Influenza	Shielding	31	0.15	(31, 31)
South Africa	Influenza	Lockdown	43	0.22	(43, 43)
South Africa	Influenza	Shielding	43	0.14	(43, 43)
Bolivia	Influenza	Shielding	48	0.20	(48, 48)
Bolivia	Influenza	Lockdown	49	0.27	(48, 50)

**Table 10: Intervention Strategies ranked by Total Hospitalisations per 100,000 Population** The result depicts the mean value over the simulation runs conducted with 95% CI and standard error.

Country	Disease-like Type	Intervention	Average Hospitalisations	SE	95% CI
United Kingdom	Influenza	Shielding	43	3.16	(37, 49)
United Kingdom	Influenza	Lockdown	52	3.36	(45, 59)
South Africa	Influenza	Shielding	67	2.12	(63, 71)
Bolivia	Influenza	Shielding	70	1.91	(66, 74)
Bolivia	Influenza	Lockdown	73	1.48	(70, 76)
South Africa	Influenza	Lockdown	76	1.54	(73, 79)
Bolivia	SARS-CoV-2	Lockdown	1828	33.48	(1762, 1894)
South Africa	SARS-CoV-2	Lockdown	1979	29.82	(1921, 2037)
Bolivia	SARS-CoV-2	Shielding	2066	20.79	(2025, 2107)
South Africa	SARS-CoV-2	Shielding	2147	19.07	(2110, 2184)
United Kingdom	SARS-CoV-2	Lockdown	3046	112.47	(2826, 3266)
United Kingdom	SARS-CoV-2	Shielding	3693	68.58	(3559, 3827)

**Table 11: Intervention Strategies ranked by Final Epidemic Size** The result depicts the mean value over the simulation runs conducted with 95% CI and standard error.

Country	Disease-like Type	Intervention	Final Epidemic Size (%)	SE	95% CI
United Kingdom	Influenza	Shielding	50.3	3.49	(43.46, 57.14)
United Kingdom	Influenza	Lockdown	59.3	3.51	(52.43, 66.17)
United Kingdom	SARS-CoV-2	Lockdown	65.0	1.97	(61.13, 68.87)
South Africa	Influenza	Shielding	76.0	2.05	(71.99, 80.01)
Bolivia	Influenza	Lockdown	77.7	1.40	(74.95, 80.45)
Bolivia	Influenza	Shielding	77.8	1.75	(74.36, 81.24)
South Africa	Influenza	Lockdown	83.6	1.45	(80.76, 86.44)
United Kingdom	SARS-CoV-2	Shielding	83.9	0.92	(82.1, 85.7)
Bolivia	SARS-CoV-2	Lockdown	86.7	0.80	(85.14, 88.26)
South Africa	SARS-CoV-2	Lockdown	89.3	0.79	(87.75, 90.85)
Bolivia	SARS-CoV-2	Shielding	94.2	0.26	(93.69, 94.71)
South Africa	SARS-CoV-2	Shielding	95.7	0.30	(95.11, 96.29)

**Table 12: Intervention Strategies ranked by Infection Fatality Ratio** The result depicts the mean value over the simulation runs conducted with 95% CI and standard error.

Country	Disease-like Type	Intervention	IFR (%)	SE	95% CI
South Africa	Influenza	Shielding	0.07529	0.00	(0.07, 0.08)
Bolivia	Influenza	Shielding	0.07606	0.00	(0.07, 0.08)
Bolivia	Influenza	Lockdown	0.07997	0.00	(0.08, 0.08)
South Africa	Influenza	Lockdown	0.08115	0.00	(0.08, 0.08)
United Kingdom	Influenza	Shielding	0.10834	0.00	(0.11, 0.11)
United Kingdom	Influenza	Lockdown	0.12448	0.00	(0.12, 0.13)
South Africa	SARS-CoV-2	Shielding	0.27676	0.00	(0.27, 0.28)
South Africa	SARS-CoV-2	Lockdown	0.27839	0.00	(0.27, 0.28)
Bolivia	SARS-CoV-2	Lockdown	0.28443	0.00	(0.27, 0.29)
Bolivia	SARS-CoV-2	Shielding	0.29280	0.00	(0.28, 0.30)
United Kingdom	SARS-CoV-2	Shielding	0.86662	0.01	(0.84, 0.89)
United Kingdom	SARS-CoV-2	Lockdown	1.01818	0.01	(0.99, 1.04)

**Table 13: Intervention Strategies ranked by Total Deaths Averted per 100,000 Population** The result depicts the mean value over the simulation runs conducted with 95% CI and standard error.

Country	Disease-like Type	Intervention	Deaths Averted	SE	95% CI
United Kingdom	SARS-CoV-2	Lockdown	387	27.12	(334, 440)
United Kingdom	SARS-CoV-2	Shielding	324	18.10	(289, 359)
Bolivia	SARS-CoV-2	Lockdown	50	6.84	(37, 63)
South Africa	SARS-CoV-2	Lockdown	30	5.19	(20, 40)
Bolivia	SARS-CoV-2	Shielding	21	5.42	(10, 32)
United Kingdom	Influenza	Shielding	20	5.02	(10, 30)
South Africa	SARS-CoV-2	Shielding	14	4.10	(6, 22)
South Africa	Influenza	Shielding	11	2.21	(7, 15)
Bolivia	Influenza	Shielding	9	2.03	(5, 13)
Bolivia	Influenza	Lockdown	6	1.62	(3, 9)
South Africa	Influenza	Lockdown	0	1.69	(-3, 3)
United Kingdom	Influenza	Lockdown	0	5.81	(-11, 11)

### **S3.3 File** - Results generated by the SEIR Model Simulations

The results for the case study can be found here: GitHub Repository: Case Study Results.

The results for the multivariate sensitivity analysis can be found here: GitHub Repository: Sensitivity Analysis (Figure 10) and GitHub Repository: Sensitivity Exchange Infectivities (Figure 11).

**S3.4 Figure** - Difference in Total Deaths per 100,000 Population between the Intervention Strategies

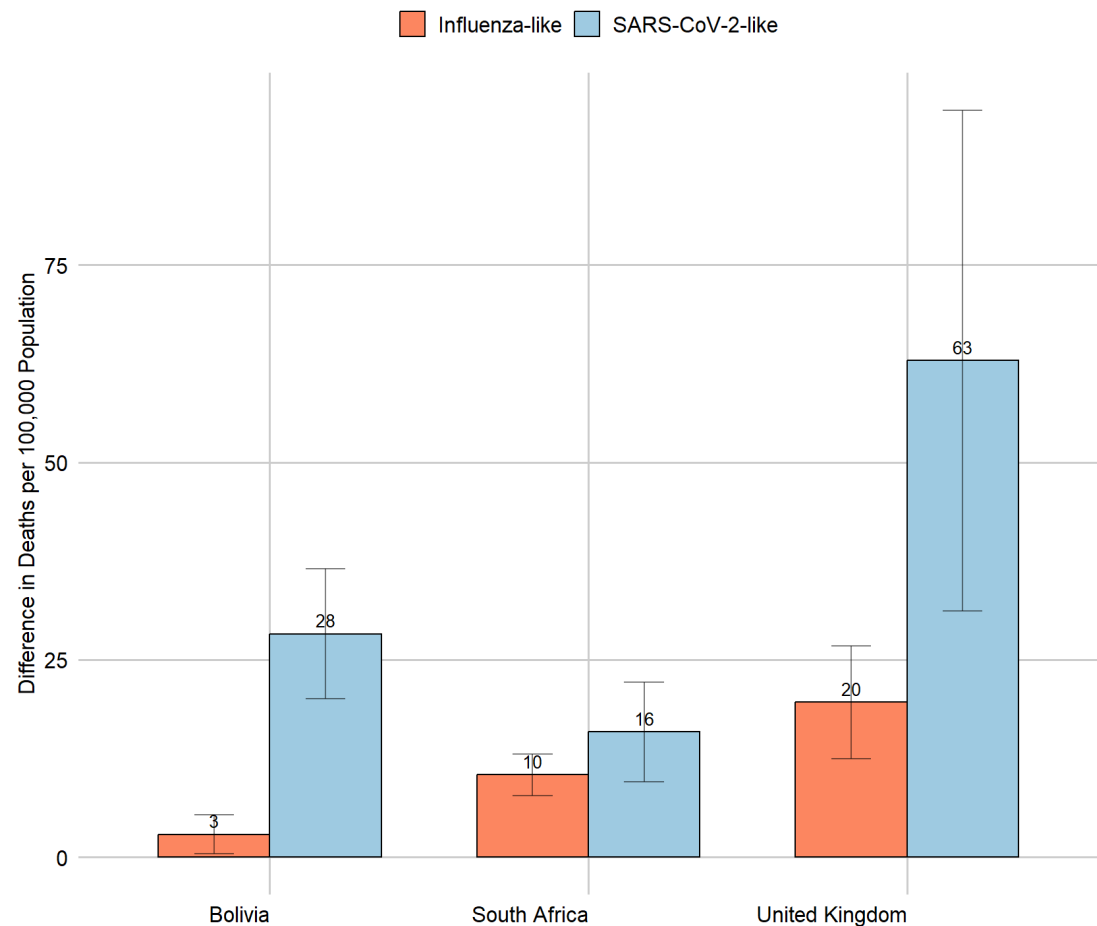


**Figure 14: Difference in Deaths per 100,000 Population Between Lockdown and Shielding Interventions Across Bolivia, South Africa** The bars represent the average difference in deaths per 100,000 for each country and disease scenario between the interventions. The error bars indicate the standard error of the difference between the two means (Lockdown and Shielding). The values used for the intervention configuration are equal to the ones depicted in Figure 9 and 8. The labels on top of each bar indicate the mean difference deaths per 100,000 population.